No. 3 1975

issued quarterly

B K

Technical Review

To Advance Techniques in Acoustical, Electrical and Mechanical Measurement

AVERAGING TIME OF RMS MEASUREMENTS

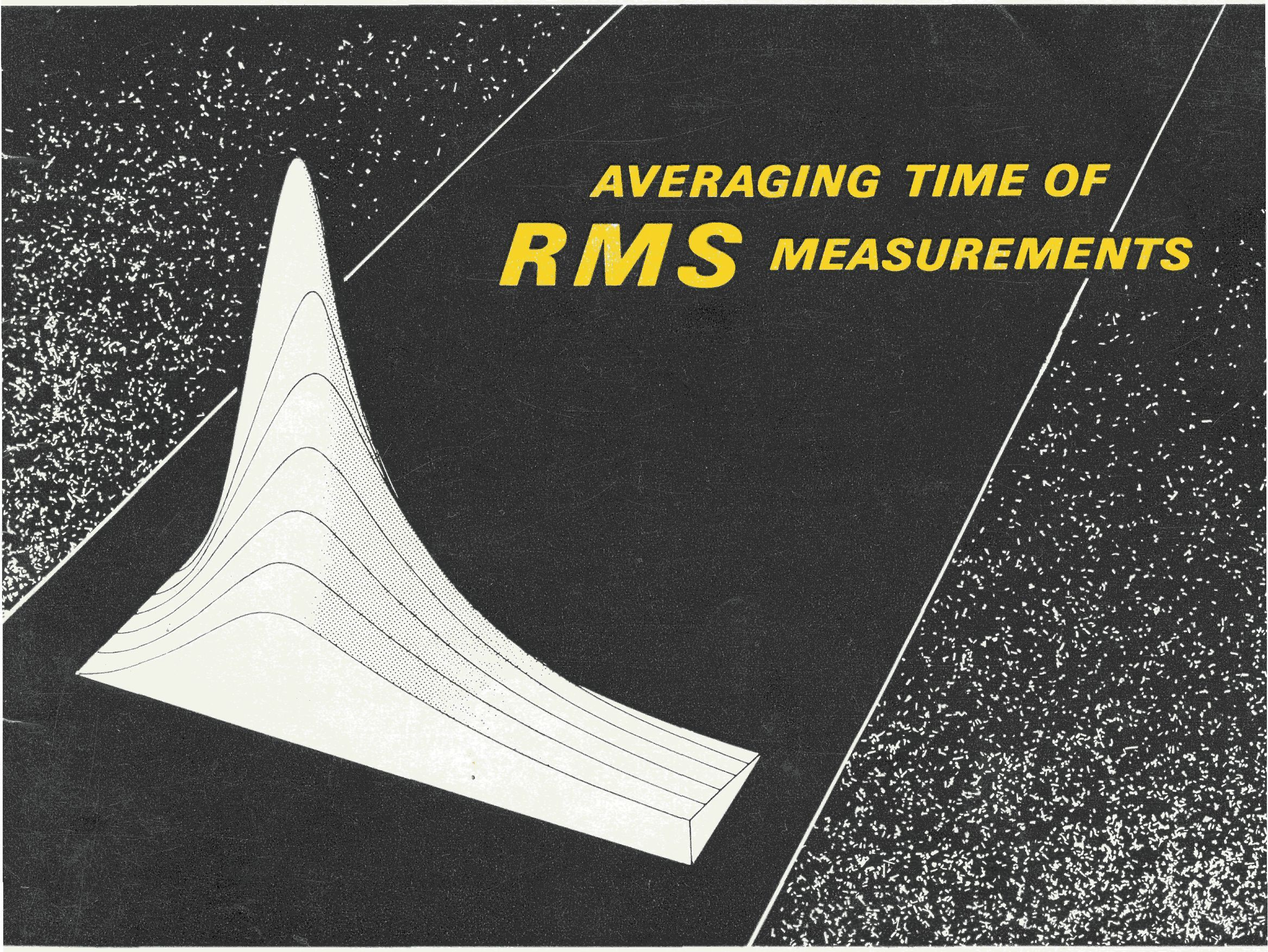

Brüel & Kjær

PREVIOUSLY ISSUED NUMBERS OF BRÜEL & KJÆR TECHNICAL REVIEW

(Continued on cover page 3)

TECHNICAL REVIEW

No. 3 — 1975

Contents

On the Averaging Time of RMS Measurements

by

C. G. Wahrmann and J. T. Broch

ABSTRACT

In the preceding B & K Technical Review (No. 2 — 1975) time averaging and/or weighting of RMS-measurements on stationary signals were discussed. The paper presented below considers the averaging of transient and impulsive as well as of sweeping sinusoidal signals. It is found that a better correlation is obtained between "running integration" and RC-weighted type of averaging of impulses if T is set equal to RC rather than 2 RC (as found for stationary signals). This is explained by the fact that in the case of impulsive signals certain definite phase relationships exist between the various frequency components of the signal.

It is concluded that general relationships of the form $T_{stat.} = 1/2\Delta f_T$ and $T_{imp.} \approx 1/h(t)_{max.}$ seem to exist where $T_{stat.}$ = Equivalent averaging time for stationary signals, $T_{imp.}$ = Equivalent averaging time for impulsive signals, and $h(t)_{max.}$ is the maximum impulse response of the time-averaging network and Δf_T is its equivalent noise bandwidth.

Finally, some practical considerations concerning existing RMS-measurement systems are outlined, particularly with regard to the socalled "direct" and the "feed-back" type RMS detecting devices.

SOMMAIRE

Dans le numéro précédant de la Revue Technique B & K (No. 2 — 1975), on a discuté l'intégration et/ou la pondération temporelles des signaux stationnaires. L'article présenté ici concerne l'intégration de signaux transitoires ou impulsionnels ainsi que celle des signaux sinusoïdaux à fréquence balayée. Il résulte de cette étude qu'on obtient une meilleure corrélation entre l'intégration continue et l'intégration à pondération RC, appliquées aux impulsions, en prenant T égal à RC plutôt qu'à 2 RC (comme c'était le cas pour les signaux stationnaires). Ceci s'explique par le fait qu'avec les signaux impulsionnels, il existe certaines relations de phase bien définies entre les différentes composantes du signal.

L'article conclut qu'il semble exister des relations générales de la forme $T_{stat.} = 1/2\Delta f_T$ et $T_{imp.} \approx 1/h(t)_{max.}$ où $T_{stat.}$ = temps d'intégration équivalent pour les signaux stationnaires, $T_{imp.}$ = temps d'intégration équivalent pour les signaux impulsionnels, $h(t)_{max.}$ = maximum de la réponse impulsionnelle du circuit d'intégration temporelle et Δf_T = bande équivalente de bruit de ce circuit.

Finalement, on met en évidence quelques considérations pratiques sur les systèmes de mesure de valeur efficace existants, en particulier en ce qui concerne les dispositifs de détection efficace dits "directs" et "à contre-réaction".

ZUSAMMENFASSUNG

In der letzten Ausgabe (TR Nr. 2 — 1975) wurde die zeitliche Mittelung und/oder Zeitbewertung bei der Effektivwertmessung stationärer Signale diskutiert. Der nachstehende Beitrag befaßt sich mit der Mittelung von flüchtigen und impulsartigen Signalen wie auch von gewobbelten Sinussignalen. Es stellt sich heraus, daß die Korrelation zwischen gleitender Integration über die Zeit T und RC — Mittelung eine bessere ist für T = RC als für T = 2 RC (wie für stationäre Signale gefunden wurde). Dies wird dadurch erklärt, daß im Falle impulsartiger Signale eine definierte Phasenbeziehung zwischen den verschiedenen Frequenzkomponenten des Signals besteht.

Es wird gefolgert, daß eine generelle Beziehung der Form $T_{stat} = 1/2\Delta f_T$ und $T_{imp.} \approx 1/h(t)_{max.}$ zu existieren scheint, wobei T_{stat} = äquivalente Mittlungszeit für stationäre Signale, $T_{imp.}$ = äquivalente Mittlungszeit für impulsartige Signale, $h(t)_{max.}$ = Maximum der Impulsantwort der Mittlungsschaltung, und Δf_T = äquivalente Rauschbandbreite.

Schließlich werden einige praktische Überlegungen zu existierenden Effektivwert — Meßschaltungen angestellt, insbesondere in Hinsicht auf "Geradeaus"-Schaltungen und solche mit Signalrückführung.

1. Introduction

As stated in the B & K Technical Review No. 2-1975 there are, basically, several ways in which the time averaging can be performed experimentally:

1. Long-time integration/averaging.
2. Step-wise integration/averaging.
3. Running integration/averaging.
4. Weighted integration/averaging.

In the case of *long-time integration*/averaging the averaging time T is chosen to equal the total time of observation of the signal.

A more practical method of integration/averaging is the *step-wise integration* mentioned above. Here the signal is integrated and averaged over a time T, whereafter a new averaging takes place over another period of time T starting at the end of the first period, etc. The result of the averaging is indicated at the end of each period T.

The third method is called *"running integration"* and consists in a true, continuous averaging over the last T seconds of the signal i.e. the integrating memory continuously "throws away" signal values which occurred before $(t - T)$.

The fourth method mentioned above, i.e. the weighted integration/averaging, is the most commonly used type of averaging to date. In analog type measuring instruments the weighting is normally exponential and is derived from R-C averaging circuits.

While the running integration/averaging weight each instantaneous value of the signal within T equally, the weighted averaging may give greater weight to signal values occurring at the instant of measurement than to signal values occurring, say T seconds earlier.

As time and frequency are dual quantities, it is possible to study the time averaging process either in the *time domain* or in the *frequency domain*. Conversion from one domain to the other is, in this case, based on the so-called Fourier-transformation and the principle of superposition.

Utilization of the superposition principle can be made for instance by considering the function $f(t)$ as consisting of an infinite number of impulses each with an infinitesimal width, $\Delta\tau$, and a height $f(\tau)$, and superimposing the responses produced by the action of each of these impulses. Mathematically this can be written:

$$x(t) = \int_{-\infty}^{t} f(\tau) h(t-\tau)\, d\tau$$

where $h(t-\tau)$ is the response of the system at the time t to a unit impulse excitation acting at time τ. A unit impulse (Dirac δ-function) excitation is characterized by the fact that it is zero, except at $t=\tau$ where it is infinite, and encloses unit area:

$$\lim_{\varepsilon \to 0} \int_{-\varepsilon}^{\varepsilon} \delta(\tau)\, d\tau = 1$$

By applying the Fourier transformation theorem to the function $x(t)$ above it can be readily shown that:

$$X(\omega) = H(\omega) \cdot F(\omega)$$

Here $X(\omega)$ is the Fourier transform of $x(t)$, $F(\omega)$ is the (complex) frequency spectrum of the time function to be averaged and $H(\omega)$ is the (complex) frequency response function of the averaging network.

An important fact, which can be seen directly from the above expressions is that a convolution (folding) in the time domain corresponds to a straight forward multiplication in the frequency domain. Similarly, a multiplication in the time domain would result in a convolution in the frequency domain.

Sections 1, 2, 3 and 4 of the paper were covered in Technical Review No. 2-1975, and discussed the RMS averaging of stationary signals. In the following the above described techniques are applied to transient and impulsive phenomena.

5. Averaging of Transient and Impulsive Signals

In dealing with the averaging of transient and impulsive signals use is, once again, made of time domain descriptions.

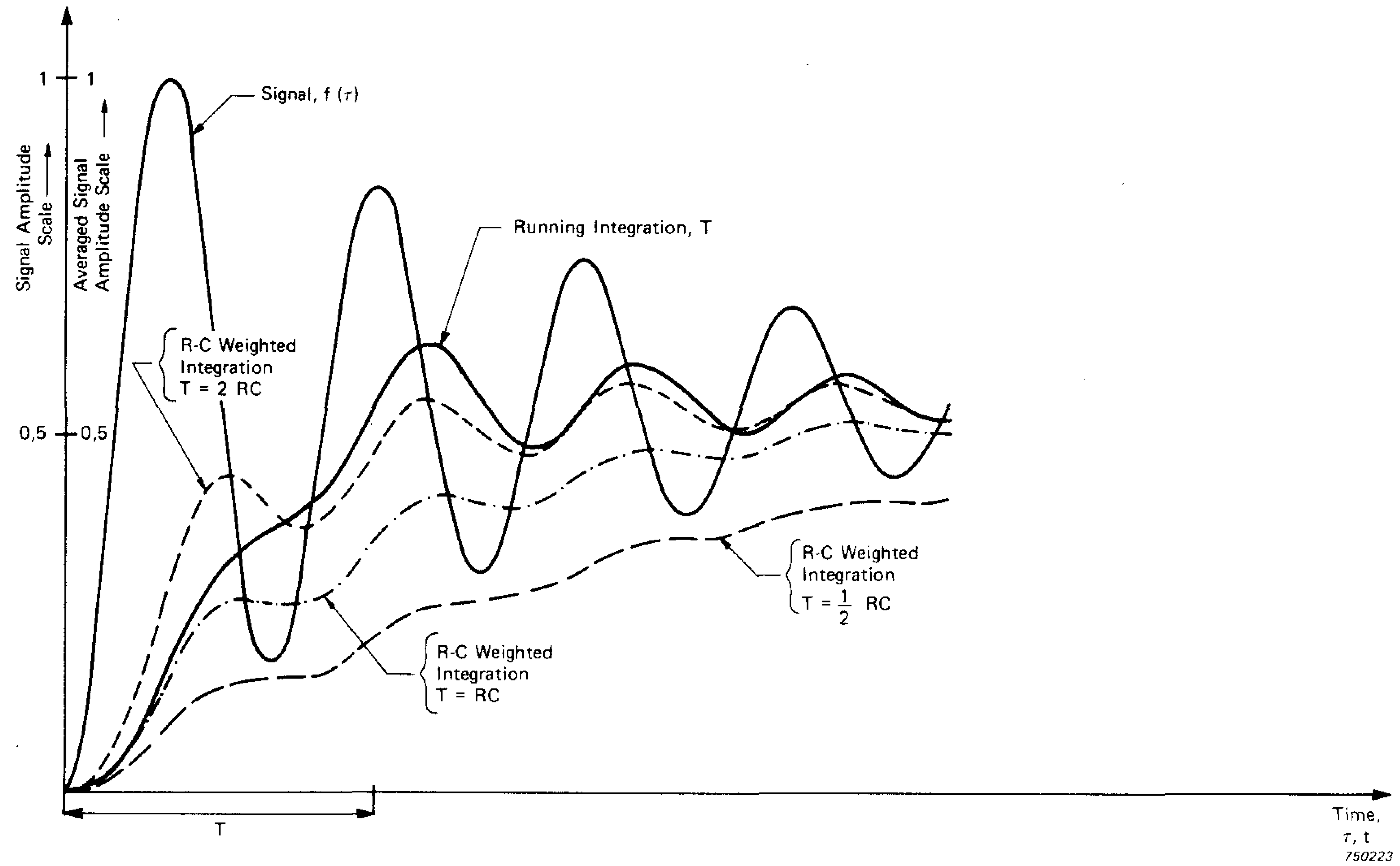

Fig. 11. Comparison of RC-weighted averaging and running integration of a transient signal (see also Fig. 1).

A typical transient signal is shown in Fig. 11, and, using the convolution integral technique demonstrated earlier in this paper, the results of running integration as well as of *RC*-weighted averaging are shown.

It is noticed that different relationships between T and RC have been evaluated and that $T = 2RC$ seems to be the most appropriate relationship with respect to slowly varying level fluctuations, i.e. in the right hand side of the curve shown. On the other hand, on the initial part of the curve (left hand side) a relationship $T = RC$ seems to be more appropriate. That this actually is so, can be further enlightened as follows:

If the signal to be averaged is a unit impulse (δ-function) occurring at $t = 0$ then the result of running integration would be:

$$\frac{1}{T}\int_{-T/2}^{T/2} \delta(\tau)\, d\tau = \frac{1}{T}$$

The result of *RC*-averaging would be:

$$\frac{1}{RC}\int_{0}^{t} \delta(\tau)\exp[-(t-\tau)/RC]\, d\tau = \frac{1}{RC}\exp(-t/RC)$$

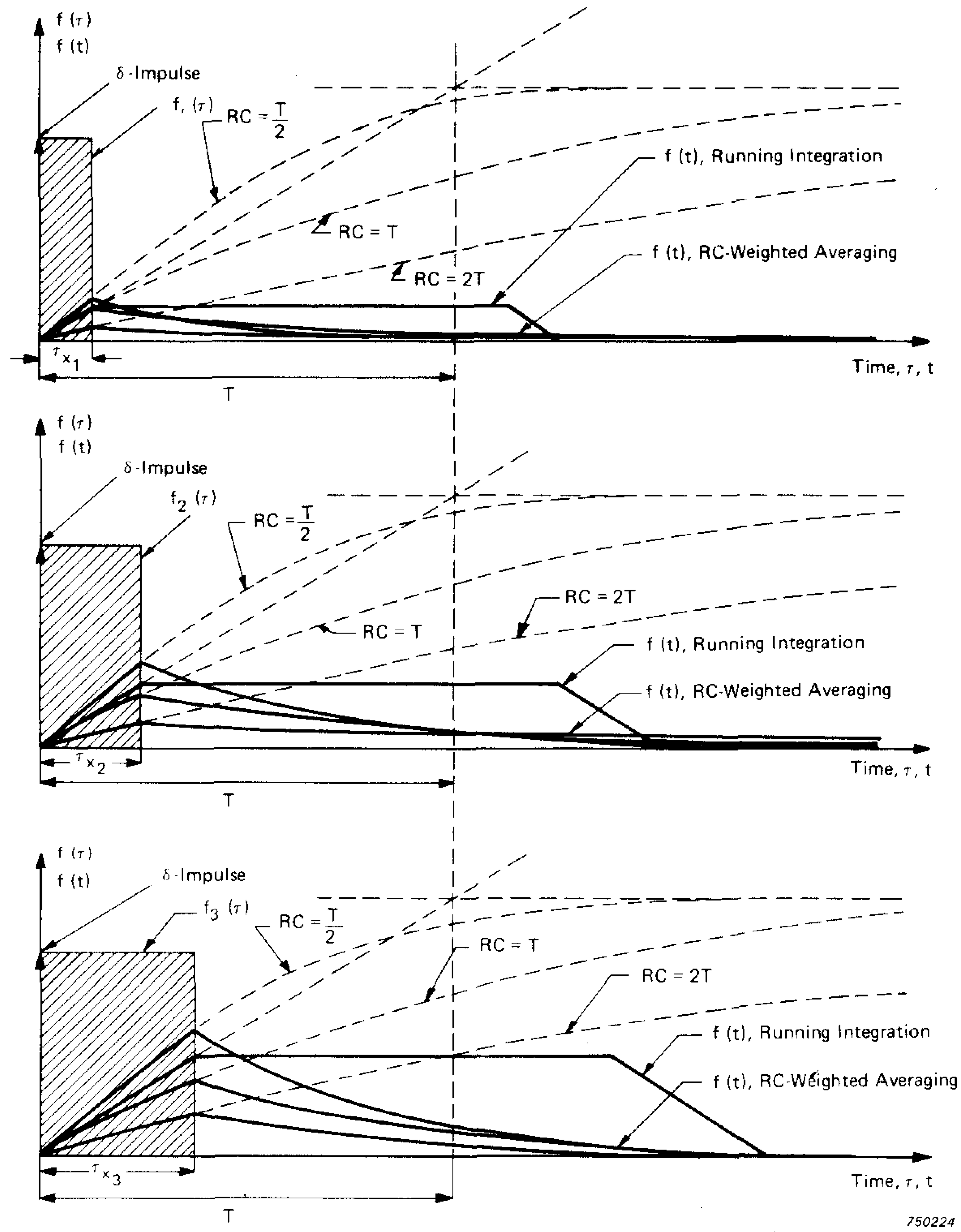

Fig. 12. Examples of integration/averaging of rectangular impulses of different width (time duration).

which, by definition, is the impulse response of the *RC*-weighting. The maximum value of the *RC*-weighting ($t = 0$) thus coincides with that of running integration when $T = RC$.

Still further light can be thrown on this behaviour of the *RC*-weighting if the δ-impulse is changed into a rectangular impulse of width τ_x, Fig. 12.

The results of running integration as well as that of *RC*-weighted averaging are indicated in the figure and again it is seen that as long as $\tau_x \ll T$ *the relationship* $T = RC$ *gives the best correlation for the "instantaneous" averaging during the duration of the pulse.*

Similar results are demonstrated in Fig. 13 with respect to a "smoothly" shaped pulse of the type:

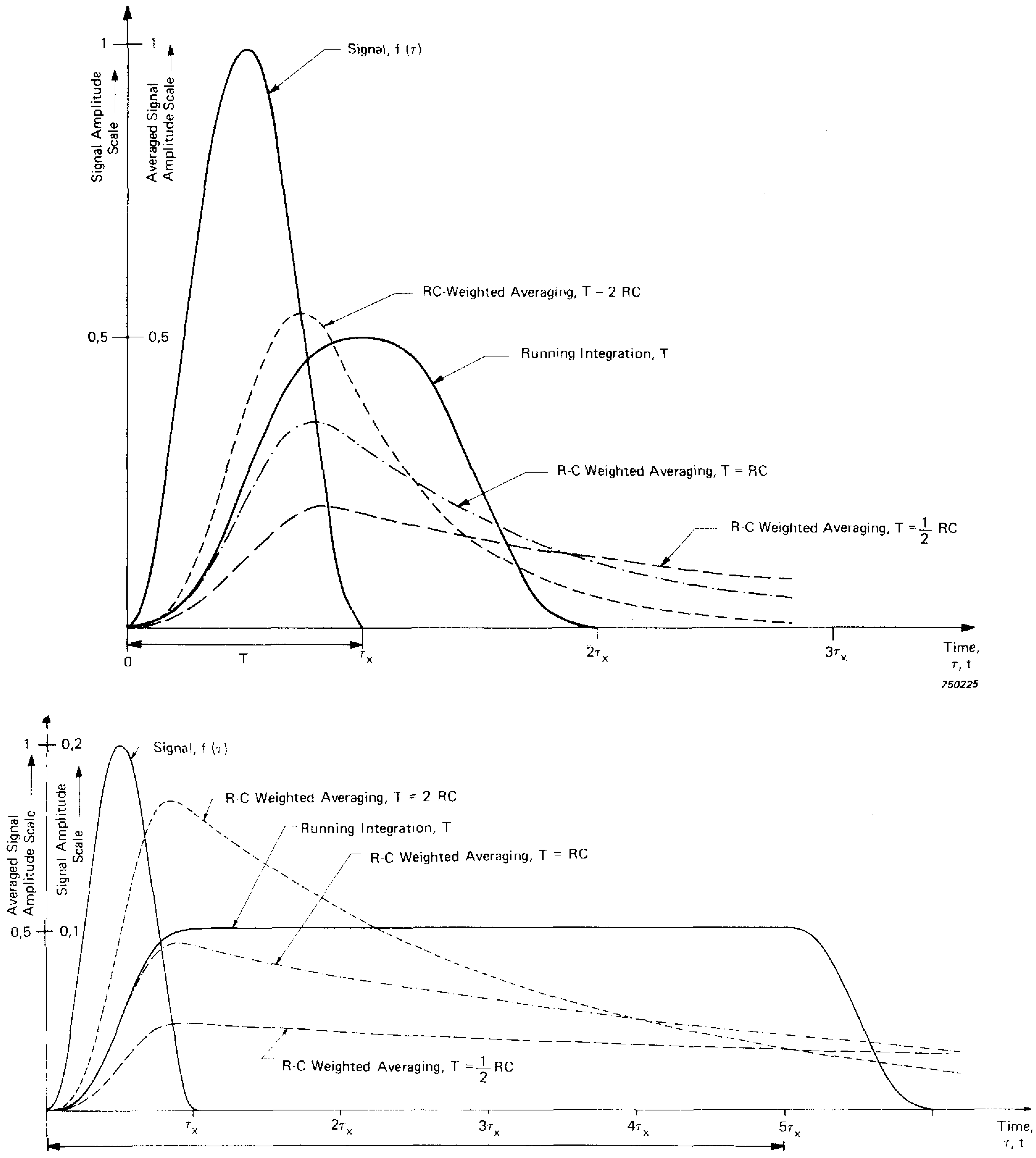

Fig. 13. Examples of integration/averaging of a smoothly shaped impulse.
a) The integration/averaging time, T, is equal to the overall impulse duration
b) The integration/averaging time, T, is equal to five times the overall impulse duration

$$f(\tau) = \frac{aX_0{}^2}{2}(1 - \cos[2\omega\tau]) \qquad 0 < \omega\tau < 2\pi$$

The behaviour demonstrated in Fig. 12 can be summarized in a chart of the kind shown in Fig. 14, which clearly indicates that the best

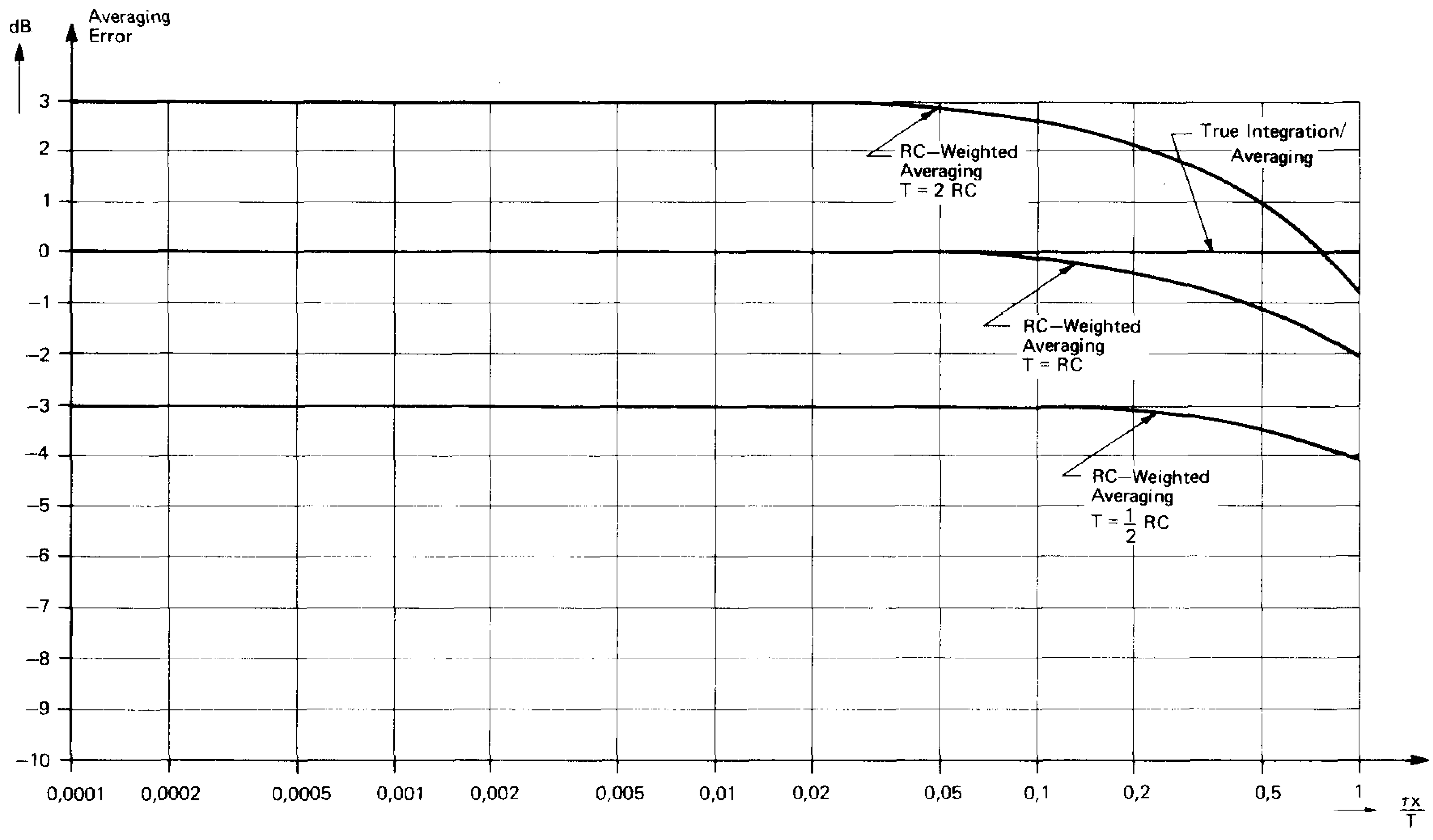

Fig. 14. Chart summarizing the deviation between true integration/ averaging and RC-weighted averaging for rectangular pulses and different relationships between T, RC and τ_x *(*$\tau_x =$ *impulse duration).*

correlation between true integration (averaging) and RC-weighted averaging for impulsive signals is obtained by setting $RC = T$ and $T \gg \tau_x$ where τ_x is the effective width of the impulse.

6. Averaging of Swept Signals

An aspect, which was touched upon earlier in this paper, and which is also very important when the properties of averaging processes are compared, is their ability to follow large changes in signal levels. Such changes occur, for instance, when frequency response characteristics of resonant, or band limited, systems are measured by means of a so-called automatic sweep technique. The automatic sweep technique may be based on wide-band response measurement to a sweeping sinewave excitation of the system, or by measuring the output from a sweeping narrow band frequency analyzer, exciting the system by means of wide band random noise. Typical results of sweeping sinewave measurements are sketched in Fig. 15.

Consider first the case of a resonant peak in the system response, such as the one marked R in Fig. 15a).

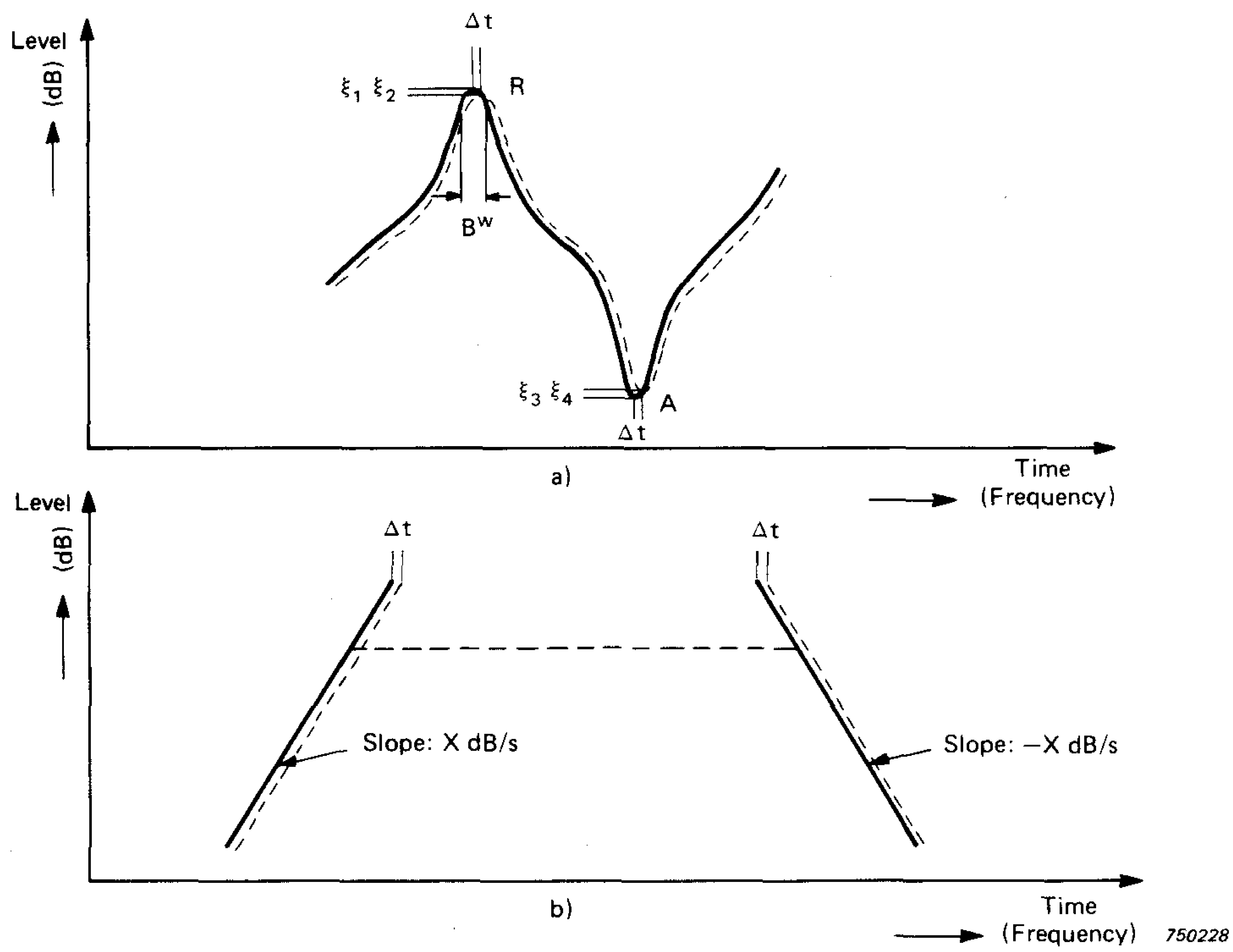

Fig. 15. Typical swept frequency response characteristics:
a) Resonant response.
b) Band-limited response.

Depending upon the sweep speed, S, the averaging time, T, and the resonance bandwidth (half-power width), BW, an error will occur in the measured response maximum. The magnitude of this error is derived theoretically in Appendix B, and the results are plotted in Fig. 16, both for the case of running integration (fully drawn curve) and for RC-weighted averaging with $T = 2\ RC$ (dotted curve).

The mathematical expression for the case of running integration is:

$$\xi_1 = \frac{BW}{TS} \tan^{-1}\left(\frac{TS}{BW}\right)$$

while the curve (dotted) for the case of RC-weighted averaging had to be evaluated numerically by means of digital computation.

It is also possible to analyze the behaviour of the two different kinds of averaging processes in the case of "valleys" in the response characteristics, marked A in Fig. 15a), assuming that the valleys are parabolic (Appendix B).

The result of the analysis for the case of running integration is:

$$\xi_3 = 1 + \frac{1}{3}\left(\frac{TS}{BW}\right)^2$$

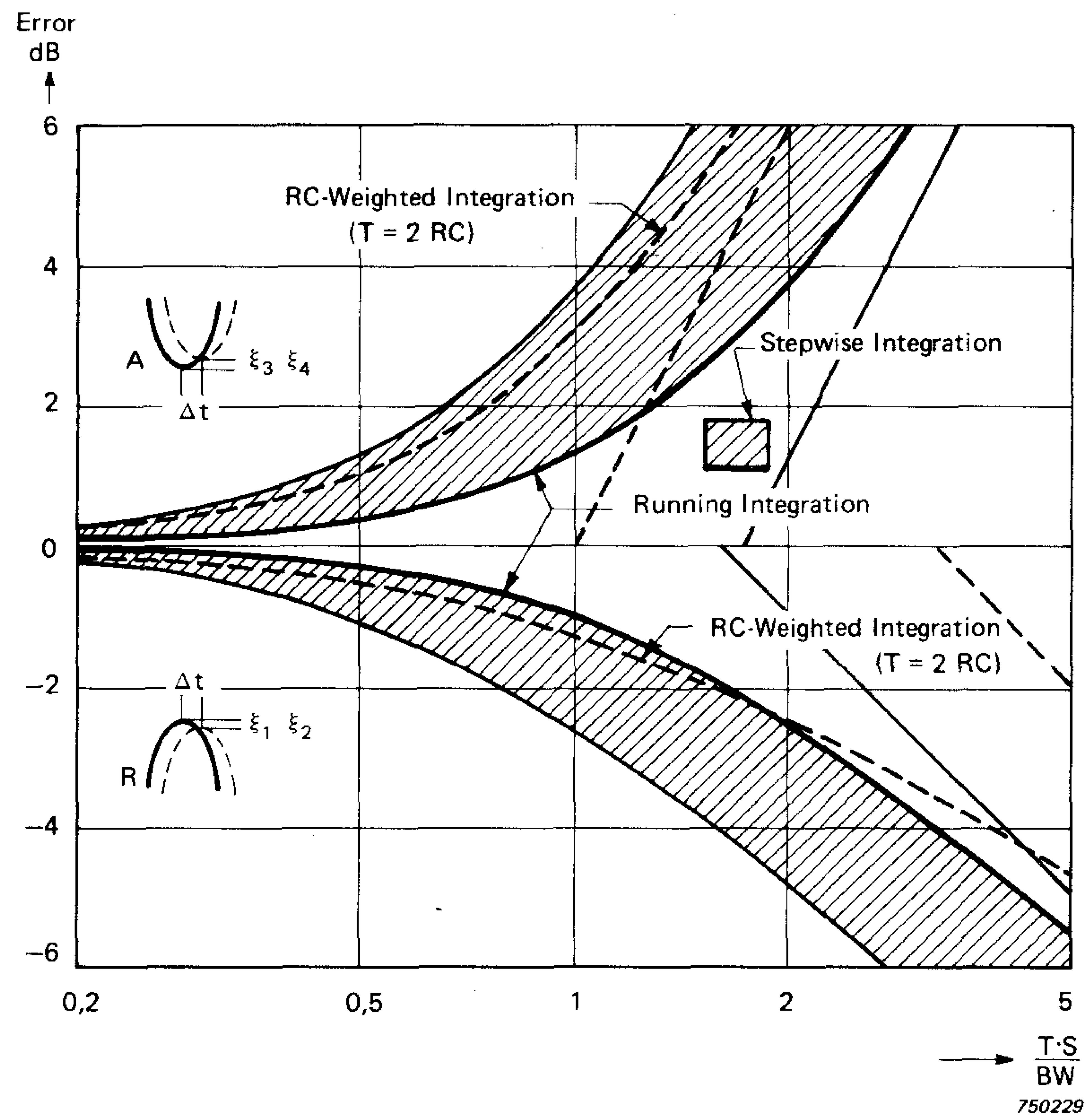

Fig. 16. Error curves for swept resonance responses (amplitudes) when various kinds of averaging techniques are used.

and for the RC-weighted averaging, again with $T = 2\,RC$:

$$\xi_4 = 1 + \left(\frac{TS}{BW}\right)^2$$

Also these results are plotted in Fig. 16.

Due to the time involved in the averaging process a certain time (frequency) delay occurs in the automatic recording of the response characteristics. This is illustrated in Fig. 15 by Δt, and analyzed in Appendix B. Fig. 17 shows the results obtained in graphical form.

One method of averaging, mentioned in the introduction to this paper and used by some manufacturers, is the so-called stepwise integration technique. The result of a stepwise integration (averaging) was illustrated in Fig. 1. The starting instants determine which parts of the time function that are averaged together. The result is the same as would be obtained by running integration/averaging followed by a sample and hold circuit. As the sampling does not necessarily happen at the maximum or minimum, further deviation will normally occur. This is also illustrated in Figs. 16 and 17 for the case of swept frequency response measurements. The worst case occurs when the maximum or minimum

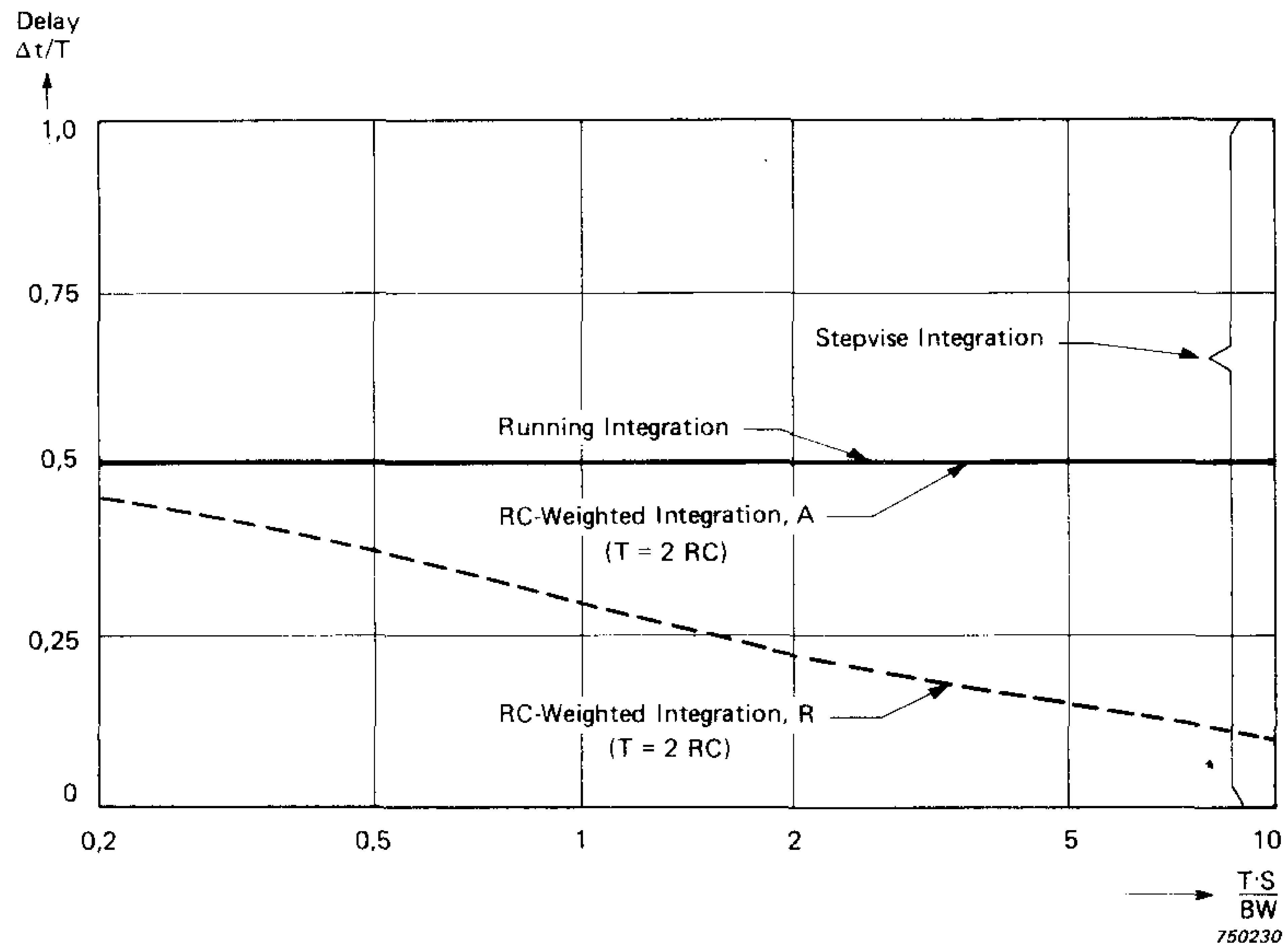

Fig. 17. Relative delays (frequency errors) for swept resonance responses when different kinds of averaging techniques are used.

is at the centre of a sampling interval, such that the two consecutive samplings show the same value. Then the error is the same as that which would be obtained by running integration with twice the averaging time.

Before leaving the subject of averaging a swept signal also the case of exponential slopes in the response should be considered, Fig. 15.

These slopes often occur when a swept, band limited, system response is measured in terms of decibels.

Mathematical descriptions of the input to the averaging circuit can in these cases be formulated as follows:

Positive slope: $f(\tau) = \exp(\alpha\tau)$

Negative slope: $f(\tau) = \exp(-\alpha\tau)$

For the sake of convenience α may be expressed in terms of *dB*/sec, i.e.:

$$X(dB/\text{sec}) = \frac{10 \log_{10}[f(\tau_2)] - 10 \log_{10}[f(\tau_1)]}{\tau_2 - \tau_1}$$

$$= \frac{10 \log_{10}[\exp(\alpha(\tau_2 - \tau_1))]}{\tau_2 - \tau_1} = \alpha \log_{10}(e)$$

or:

$$\alpha = \frac{X}{4.34}$$

Considering first the case of *positively sloping responses*:

a) Running Integration:

$$\varepsilon_1(t) = \frac{1}{T}\int_{t-T}^{t} \exp(a\tau)\, d\tau = \frac{\exp(at)}{aT}\,(1 - \exp(-aT))$$

The integrated (averaged) signal is, as indicated above, lagging behind the actual signal level because of the integration process. The value that the signal level had at an instant of time t, is reached at the output from the averager at a time t_2 given by:

$$\frac{\exp(at_2)}{aT}\,(1 - \exp(-aT)) = \exp(at_1)$$

and the "delay" time $\Delta t = t_2 - t_1$ can be found from:

$$\exp(a(t_2 - t_1)) = \exp(a\,\Delta t) = \frac{aT}{1 - \exp(-aT)}$$

and the *relative delay time* $\Delta t/T$ is:

$$\frac{\Delta t}{T} = \frac{\ln(aT) - \ln(1 - \exp(-aT))}{aT}$$

or

$$\frac{\Delta t}{T} = 4.34\,\frac{\ln(X_T/4.34) - \ln(1 - \exp(-(X_T/4.34))}{X_T}$$

where $X_T = X \cdot T$ *dB* per averaging time, T.

This function is plotted in Fig. 18 (fully drawn curve).

b) *RC-Weighted Averaging*:
Using the convolution techniques (time domain descriptions) then:

$$\varepsilon_2(t) = \frac{1}{RC}\int_{-\infty}^{t} \exp(a\tau)\exp[-\,(t-\tau)/RC]\; d\tau$$

$$= \frac{\exp(-t/RC)}{RC}\int_{-\infty}^{t} \exp((a + 1/RC)\tau)\; d\tau$$

$$\varepsilon_2 = \frac{\exp(at)}{1 + aRC}$$

With the same reasoning as above one obtains:

$$\exp(at_2)\cdot\frac{1}{1 + aRC} = \exp(at_1)$$

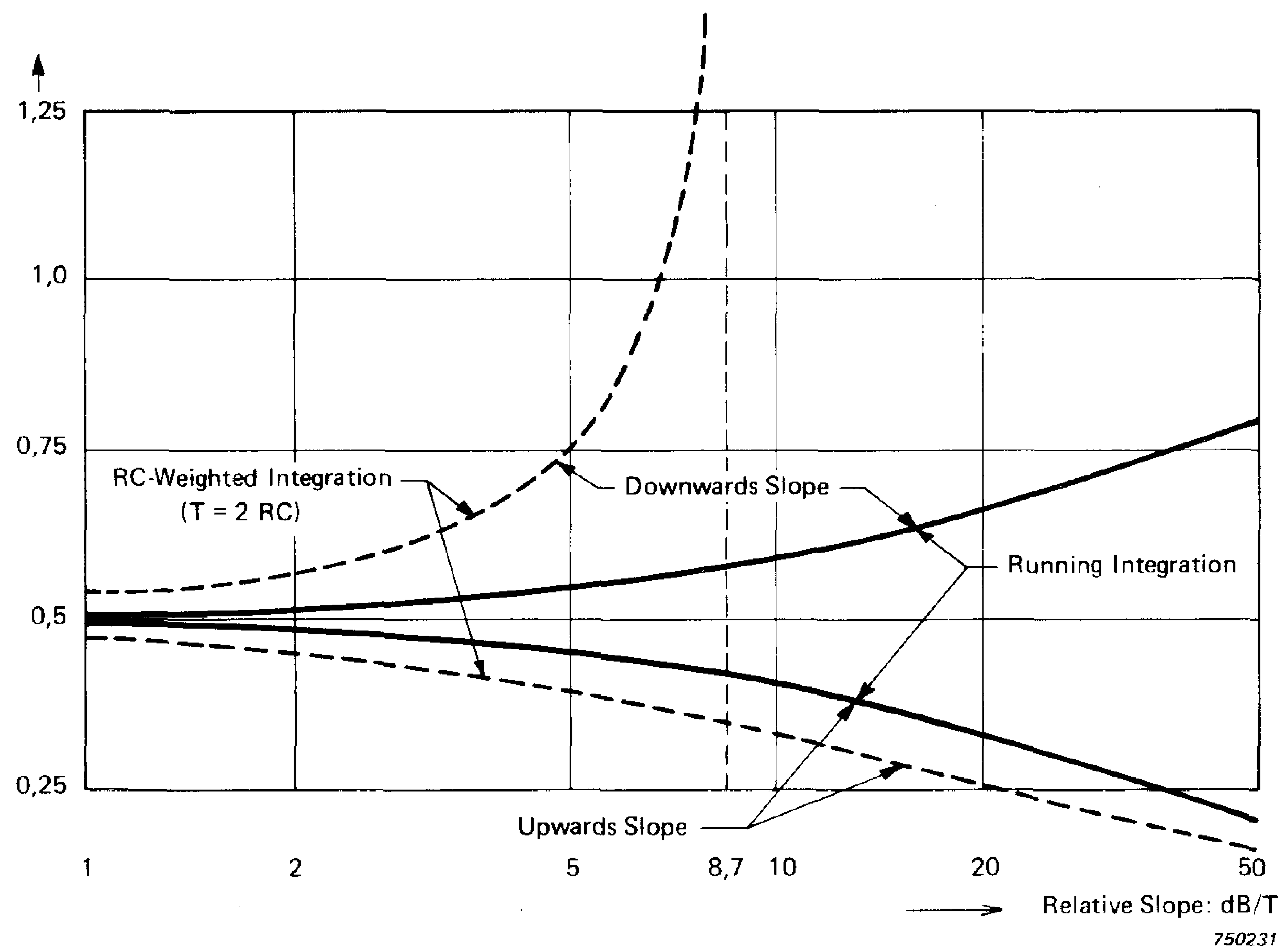

Fig. 18. Relative delays (frequency errors) when swept, band-limited frequency responses are measured and averaged by means of either running integration or RC-weighted averaging techniques.

and, using the relationship $T = 2RC$:

$$\frac{\Delta t}{T} = \frac{\ln(1 + aT/2)}{aT} = \frac{4.34}{X_T} \ln\left(1 + \frac{X_T}{8.7}\right)$$

The function is plotted in Fig. 18 (dotted curve) and it is seen that the relative delay for *R-C*-weighted averaging of positively sloping signal levels is smaller than when the running integration technique is used, cfr. also Fig. 17.

Considering next the case of *negatively sloping responses*:

a) *Running Integration*:

$$\frac{\Delta t}{T} = 4.34 \frac{\ln[\exp(X_T/4.34) - 1] - \ln(X_T/4.34)}{X_T}$$

See Fig. 18 (fully drawn curve).

b) *RC-Weighted Averaging*:

$$\frac{\Delta t}{T} = -\frac{4.34}{X_T} \ln\left(1 - \frac{X_T}{8.7}\right)$$

Also this function is plotted in Fig. 18 (dotted curve) and it is noticed that for *negatively sloping responses with slopes of* 8.7 *dB/Averaging Time, and larger, the RC-weighted averaging cannot follow signal level changes and infinite delays (and errors) occur.*

7. General Theoretical Conclusions. Use of other than RC-Weighting Functions

In the preceding text a relatively extensive treatment has been given of the use of so-called running integration and RC-weighted averaging techniques, as these techniques are of great practical importance. A number of phenomena were considered individually and it may therefore be timely at this stage to summarize the results and to extend the general findings to other kinds of weighted averaging techniques.

It was found that when measurements are made on stationary random signals RC-weighted averaging can be compared directly with running integration when a relationship of the kind $T = 2\,RC$ is used.

This relationship was also found to be a good compromise when dealing with stationary periodic signals. However, in the case of impulsive signals a relationship of the kind $T = RC$ was found to be more appropriate.

Furthermore, it could be concluded that the measurement errors (or fluctuations) in the above mentioned cases become less the larger one chooses T, a fact which is fairly obvious from a physical point of view.

Now, how come that *there is a definite theoretical difference in "equivalent averaging time" whether measurements are made on stationary or impulsive signals*? The answer to this question lies in the fact that when impulsive signals are applied to the averaging system not only the magnitudes but also the relative phases of the signal frequency components become important for the measurement, even if the signal is squared before averaging. Another way of answering the same question is to consider the fact that when stationary signals are measured the measuring instrument indicates a *stationary* average value, while in the case of impulsive signals a *peak* "average" is measured.

Returning to the case of stationary signals the results obtained in section 3) of this paper can be readily generalized to give a relationship of the form:

$$T_{stat} = \frac{1}{2\,\Delta f_T}$$

where Δf_T is the equivalent noise bandwidth of the averaging system. The relationship is exact for the case of band-limited, stationary random noise and represents an acceptable compromise for stationary periodic signals with constant or slowly changing signal levels.

For the case of single impulses the concept of "equivalent noise bandwidth" cannot be applied to the problem directly. Here actually the impulse response of the averaging system must be considered. Although the impulse response of a system is related to the system bandwidth no simple general relationship can, however, be formulated. The actual relationship depends not only upon the bandwidth but also upon several other parameters.

A simple *RC*-weighted system as shown in Figs. 3 and 19a) is commonly termed a first order system. The impulse response function of this system is also shown in Fig. 19a).

Another type of averaging system is shown in Fig. 19b), together with its impulse response function. This type of system is termed a "higher order" system as it contains more components than the simple *RC*-system. (Actually the system shown is a fifth order filter of the Butterworth type). Now, the maximum response (peak response) of an averaging system to an impulse, the duration of which is *very much* shorter than the system response time (δ-impulse) is equal to the maximum impulse response times the time integral of the impulse i.e.:

$$f(t)_{\max} = h(t)_{\max} \int_{\substack{\text{over the}\\ \text{impulse}}} F_\delta(\tau)\, d\tau$$

(This is a strictly hypothetical consideration. Theoretically the actual maximum response should be found by convolution, and deviations from the above statement occur. As will be shown below, however, the expression allows an "optimum equivalent" averaging time for impulse measurements to be defined which is practically useful).

If the averaging system is of the true ("running") integration type, then

$$f(t)_{\max} = \frac{1}{T} \int_{\substack{\text{over the}\\ \text{impulse}}} F_\delta(\tau)\, d\tau \qquad T \gg \tau_x$$

and a general relationship of the form:

$$T_{\text{imp}} \approx \frac{1}{h(t)_{\max}}$$

can be formulated.

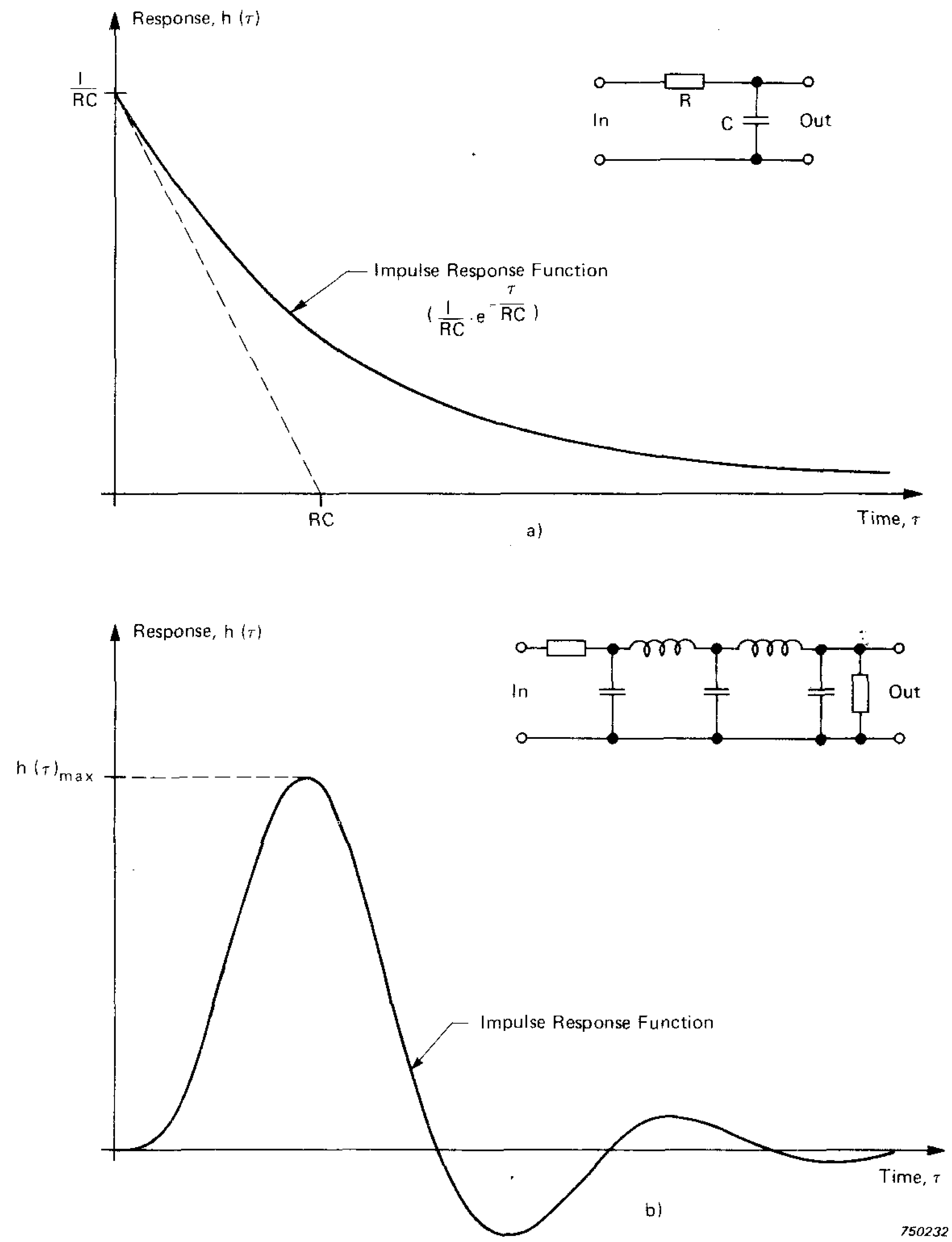

Fig. 19. Examples of weighting networks used in analog averaging systems, together with their respective impulse response functions.
a) A simple RC-type of weighting network.
b) A higher order weighting network of the Butterworth type.

It was stated above that for this relationship to hold true the impulse should be of the δ-impulse type. This is theoretically so. In practice, on the other hand, it is only required that the maximum impulse response should be approximately flat over the period of time during which the impulse exists, a condition which is illustrated in Fig. 20.

As an example of the use of the above expression consider RC-weighted averaging as illustrated in Fig. 19a).

$$T_{imp} \approx \frac{1}{h(t)_{max}} = RC$$

and $T \gg \tau_x$.

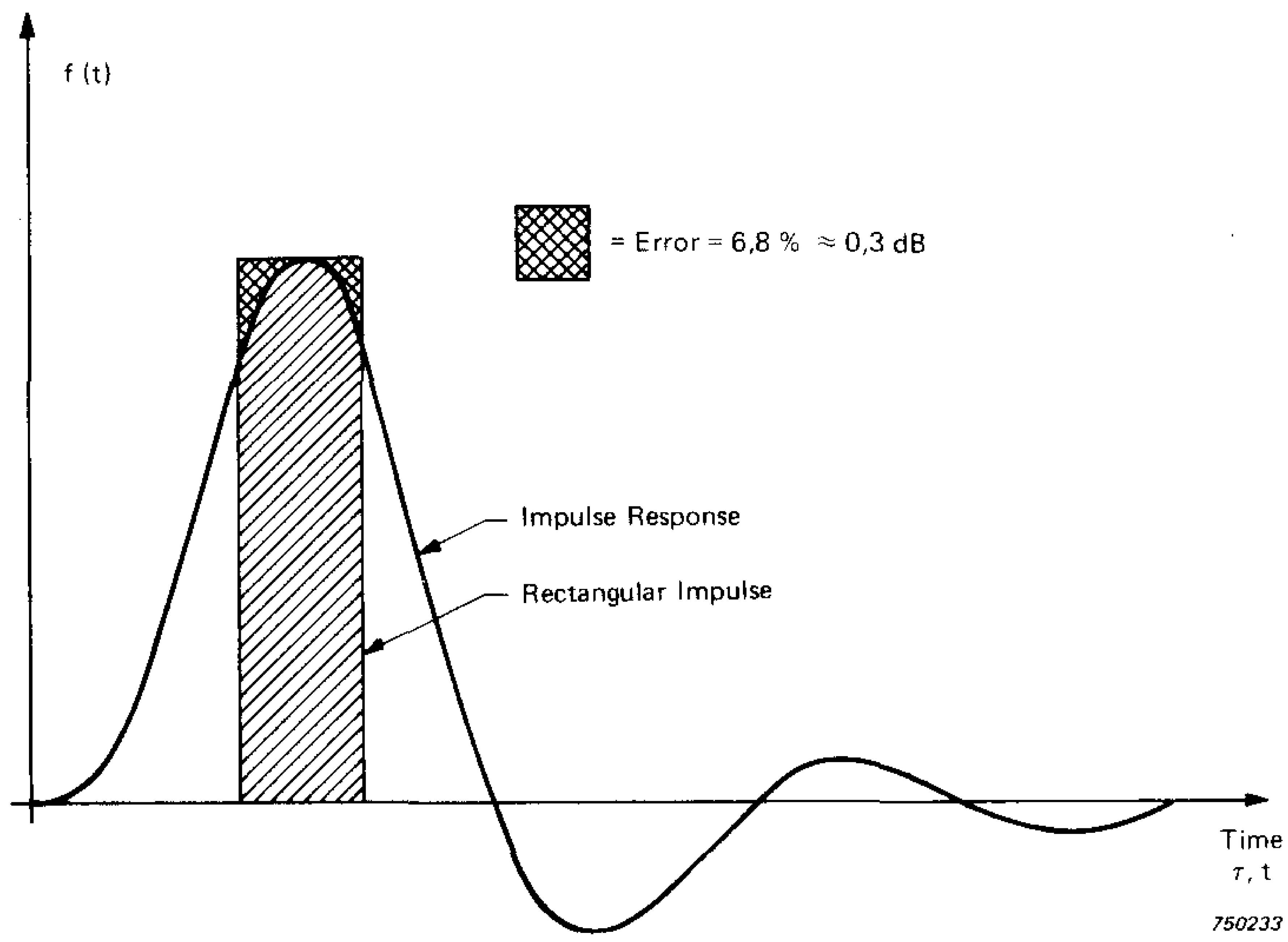

Fig. 20. Sketch illustrating the approximate maximum response of an averaging system to "short" duration impulses.

The condition $T \gg \tau_x$ should be studied separately for each type of averaging system. In the case of RC-weighted averaging the impulse response function has a very sharp maximum, and to obtain only small errors T should be of the order of say ten times the impulse duration.

For higher order averaging systems, which possesses a "rounded" impulse response maximum (Fig. 19b)), T may only need to be some 3 to 5 times τ_x to obtain small errors. In the limiting case of true integration, where $h(t)_{\max}$ is flat over the complete period of averaging ($h(t)_{\max} = 1/T$). T needs actually only be *equal* to τ_x.

Before closing the discussion of the expression

$$T_{\text{imp}} \approx \frac{1}{h(t)_{\max}}$$

it should be noted that although $h(t)_{\max}$ is a response quantity it depends, as mentioned earlier, on the bandwidth of the averaging filter so that $h(t)_{\max} \propto \Delta f$.

An interesting result, obtained in section 6) of this paper, clearly demonstrates the transition from "stationary" averaging to "impulsive" averaging with regard to RC-weighted integration. This is the case of swept resonance responses. When the sweep speed is very low (TS/BW small) the swept resonance response represents a slowly changing stationary input to the averager, while at very high sweep speeds (TS/BW large) it represents an impulsive input. To

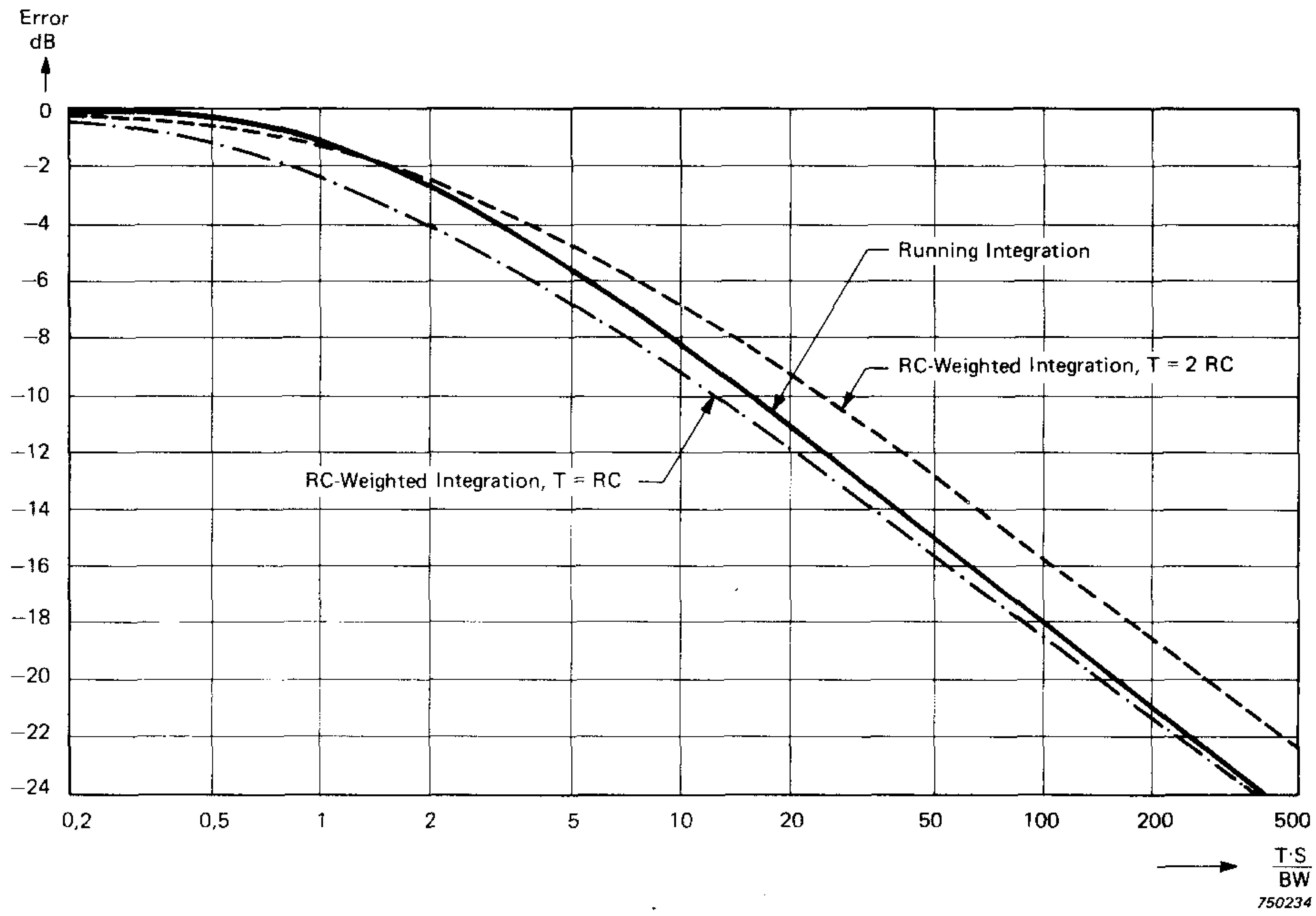

Fig. 21. Error curves for swept resonance responses (amplitudes). See also Fig. 16.

illustrate this fact the part of Fig. 16 representing swept peak *resonant* responses are redrawn in Fig. 21, together with the error curve for $T = RC$. As was to be expected for large values of TS/BW $T = RC$ becomes a better approximation to running integration than $T = 2\ RC$.

8. Some Practical Considerations

Up to this point the averaging processes considered have been applied to *ideally* squared signals.

Practical analog *RMS*-detectors do normally not perform ideal squaring, and various kinds of limitations occur which should be kept in mind when RMS-measurements are made.

The most commonly used method of realizing the squaring process in practice is to approximate the required parabolic input/output relationship of the squarer by piecewise linearization of the required parabola, Fig. 22. This approximation techniques may again take two major forms: 1) A direct approximation, to which the result obtained in this paper apply directly, and 2) A feedback type of approximation where the result must be slightly modified, as explained in this section of the paper.

In the direct type of approximation the squared signal is averaged and the square-root is extracted on the instrument meter scale. In

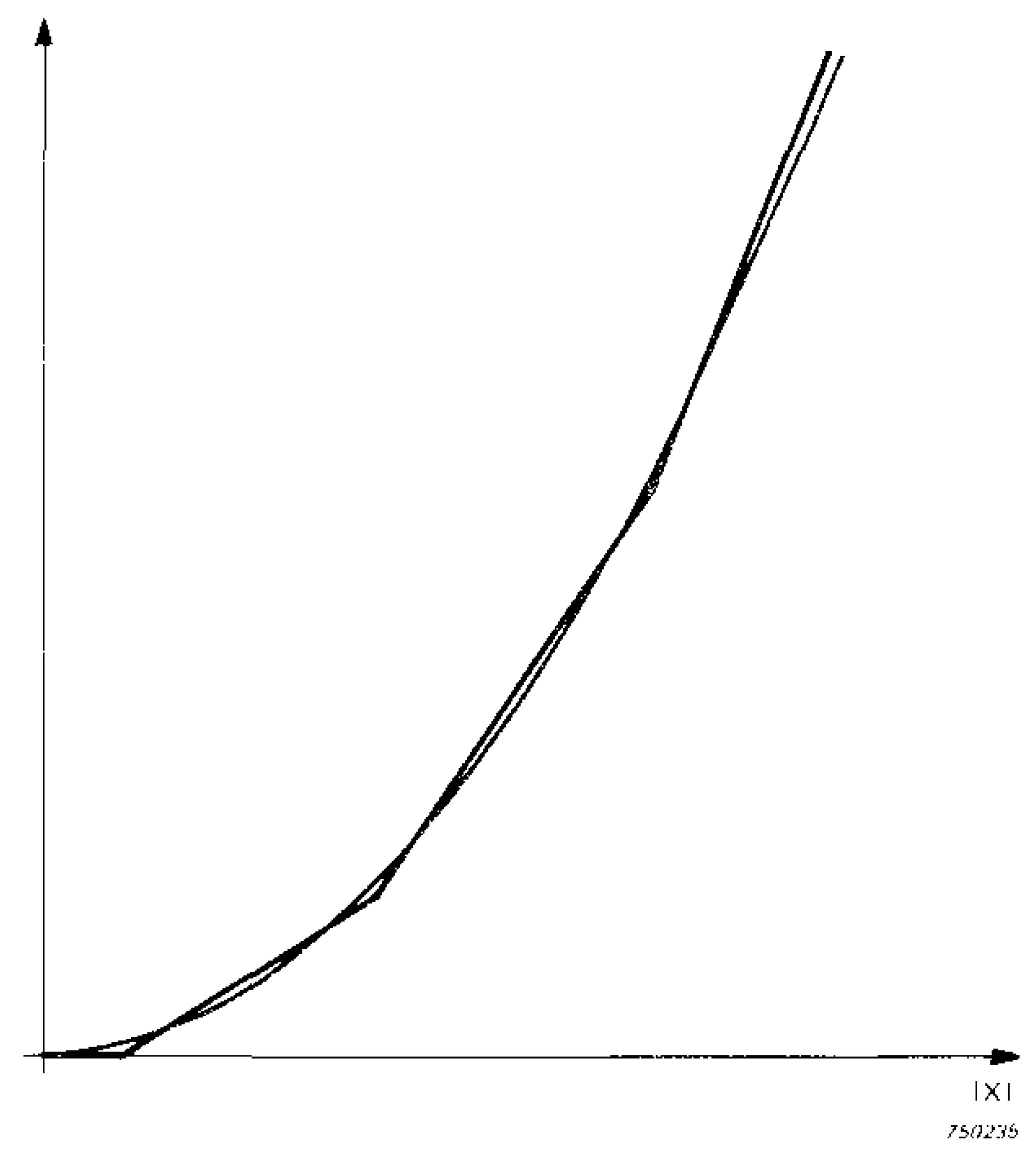

Fig. 22. Sketch illustrating the piecewise linearization of a parabola. (For further explanation see Appendix C.)

other words, the *RMS*-value is found by squarerooting the mean-square (*MS*) value:

$$RMS = \sqrt{MS}$$

In the feedback type of approximation the *RMS*-value is found by feeding a voltage proportional to the output (*RMS*-value) back into the squaring device, i.e.:

$$RMS = \frac{MS}{RMS} = \sqrt{\frac{(MS)^2}{MS}} = RMS$$

This method was first introduced by one of the authors (Wahrman, 1958) and has been extensively used by Brüel & Kjær.

The major limitations of the direct method lie in dynamic range considerations, while the major limitation of the feedback method is determined by the crest-factor †) capability of the detector circuit.

A great advantage of the feedback method is that a linear instrument meter scale is obtained, see also Appendix C.

If the input signal is stationary and its crest-factor is below some value specified for the squaring circuit the results obtained from measurements using the feedback type of approximation, and those obtained from measurements using the direct type of approximation, are identical.

---

† Crest-factor $= \frac{\text{Signal Peak Value}}{\text{Signal RMS-Value}}$

In the case of single impulses, however, the two types of detectors behave differently. As long as the signal (impulse) is within the dynamic range of the detector the output from the direct approximation type circuit is a mean square value, which results in (impulsive) *RMS*-value of the expected type.

In the case of the feedback type of approximation, on the other hand, the impulse will actually not be squared when its duration is less than approximately T/C^2 where T is the averaging time and C is the crest-factor capability of the circuit ($C = \sqrt{T/\tau_x}$).

When τ_x is much smaller than T/C^2 the feedback type squaring circuit acts as an average absolute detector and no squaring of the signal takes place.

On the basis of these considerations, and discussions earlier in this paper, practical error-curves for true integration/averaging, as well as for *RC*-weighted averaging with $RC = T$, can be deduced for *RMS* measurements on single, rectangularly shaped, impulses. The result is shown in Fig. 23, and it may be concluded that for instruments with crest-factor capabilities of say 10 and *RC*-weighted averaging proper *RMS* measurements can only be made if the impulse duration is in the region:

$$0{,}03T < \tau_x < 0{,}3T \quad \text{(Error of the order of 0,5 dB or less.)}$$

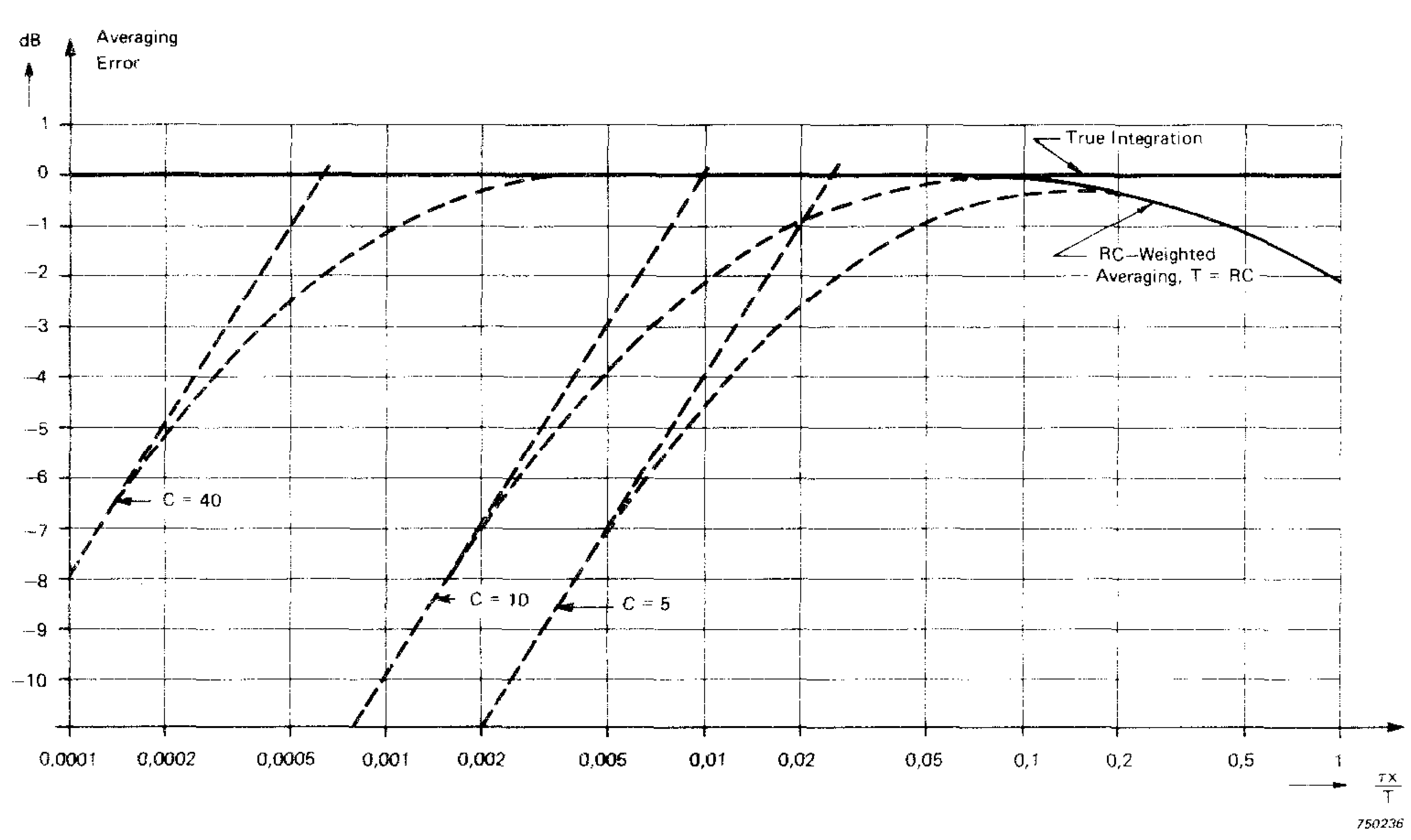

Fig. 23. Practical error curves for measurements on single, rectangularly shaped impulses of duration τ_x. Note the influence of the crest-factor capability of the squaring device.

At this stage it should be mentioned that the crest-factor capability of feedback type squaring devices, in general, is independent upon the actually measured *RMS*-value, while in the case of direct type devices it depends directly upon where in the dynamic range (and meter range) the *RMS*-value lies.

Another, very important, difference between the direct type of squaring device and the feedback type, is the difference in effective *RC*-value in the averaging process of the two cases. This difference is derived and discussed in Appendix C, and it is shown that *in the case of feedback type squaring devices the actual RC-value is twice that of the RC-value of the equivalent direct type devices*. Thus applying the preceding theory of *RC*-weighted averaging to measurements with a feedback type squaring device *RC* should be substituted by (*RC*) Feedback where:

$$(RC)_{\text{feedback}} = 2(RC)_{\text{direct}}$$

In this section on practical considerations it should also be mentioned that when the averaging time is relatively short, say $T < 1$ sec different effective averaging may be obtained whether the result is read on the instrument meter or directly across the capacitor in the averaging network (DC-output). The reason for the differences lies in the fact that if the result is read on the instrument meter the effective averaging network is no longer of the simple *RC*-type, but includes the network properties of the meter itself, see also Appendix C.

9. Summary of Results

In this paper the subject of averaging time in *RMS*-measurements has been discussed in quite some details. Error curves have been derived for typical practical cases using what has been termed "running integration" and "*RC*-weighted averaging" techniques. However, it has also been found possible to formulate some more general relationships between the mathematically proper "running integration" averaging time, *T*, and the properties of analog weighting networks.

It was found that for *constant, or slowly varying, signal levels a relationship* of the form

$$T_{\text{stat}} = \frac{1}{2\,\Delta f_T}$$

where Δf_T is the equivalent noise bandwidth of the (analog) averaging system, could be formulated. In case measurements are to be made on *impulsive signals*, such as single impulses, the " optimum " relationship between the (theoretical) averaging time T, and the properties of the analog weighting network takes a somewhat different form, namely:

$$T_{imp} \approx \frac{1}{h(t)_{max}}$$

where $h(t)_{max}$ is the maximum unit impulse response of the network.

If the weighting network considered is of the RC-type, then in particular:

$$T_{stat} = 2(RC)_{direct} \quad \text{and} \quad T_{imp} = (RC)_{direct}$$

Finally, some practical considerations have been outlined regarding dynamic range, crest-factor capabilities, squaring devices, and readout characteristics of commercially available instruments.

References

1. BROCH, J. T. and WAHRMAN, C. G.: Effective Averaging Time of Level Recorders. Brüel & Kjær Technical Review No. 1-1961.
2. WAHRMAN, C. G.: A True RMS Instrument. Brüel & Kjær Technical Review No. 3-1958.
3. WAHRMAN, C. G.: Methods of Checking the RMS Properties of RMS Instruments. Brüel & Kjær Technical Review No. 1-1963.
4. WAHRMAN, C. G.: Impulse Noise Measurements. Brüel & Kjær Technical Review No. 1-1969.
5. RICE, S. O.: Mathematical Analysis of Random Noise. Bell System. Techn. Journal 23 (1944) and 24 (1945). Also contained in N. Wax.: " Selected Papers on Noise and Stochastic Processes ". Dover Publications, Inc. New York 1954.

APPENDIX B

Averaging of Swept Resonant Response Functions
In order to analyze the actual behaviour of the averaging process for the case of swept resonant response functions consider first the case of a resonant "peak" (marked R in Fig. 15a) of the main text.

At the input to the averager the resonant peak will take form of a pulse, Fig. B1, enveloping a high (variable) frequency. Assuming that the time constants involved in the averaging are much larger than the period of the high frequency only the envelope (pulse) will be of interest in the analysis to follow.

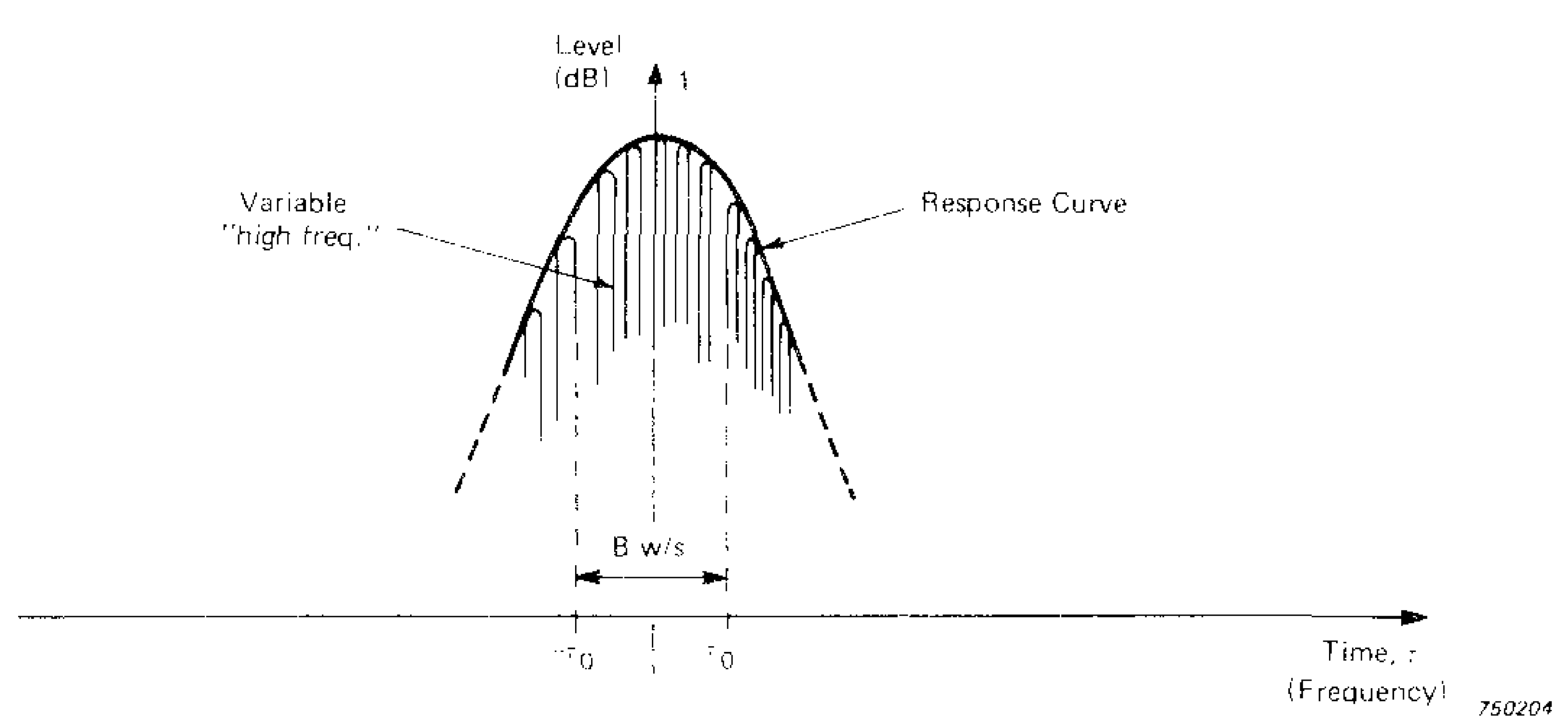

Fig. B.1. Detailed sketch of the time function output from a swept resonance response "maximum".
(Note that $2\tau_0$ is set equal to BW/S).

If the half-power bandwidth of the resonance is termed BW (Hz) and the sweep speed of the measurement system is S Hz/sec the "half-power" width of the pulse is:

$$\tau_{BW} = \frac{BW}{S} \text{ sec.}$$

Choosing the time axis for the analysis so that $\tau = 0$ coincides with the pulse maximum, and normalizing the pulse maximum to 1 (Fig. B1) the input to the averager can be written

$$f(\tau) = \frac{1}{1 + \tau^2}$$

or making the x-axis relative to τ_0 where $\tau_0 = BW/2S$ then:

$$f\left(\frac{\tau}{\tau_0}\right) = \frac{1}{1 + (\tau/\tau_0)^2}$$

If the averaging process is of the running integration type:

$$\xi_1\left(\frac{t}{\tau_0}\right) = \frac{\tau_0}{T}\int_{(t-T)/\tau_0}^{t/\tau_0} \frac{d(\tau/\tau_0)}{1 + (\tau/\tau_0)^2}$$

Thus:

$$\xi_1\left(\frac{t}{\tau_0}\right) = \frac{\tau_0}{T}\left[\tan^{-1}\left(\frac{t}{\tau_0}\right) - \tan^{-1}\left(\frac{t-T}{\tau_0}\right)\right]$$

The maximum of this function occurs when:

$$\frac{d\xi_1}{d(t/\tau_0)} = 0$$

whereby:

$$\frac{\tau_0}{T}\cdot\frac{1}{1 + (t/\tau_0)^2} - \frac{\tau_0}{T}\cdot\frac{1}{1 + ((t-T)/\tau_0)^2} = 0$$

which gives:

$$\frac{t}{\tau_0} = \frac{T}{2\tau_0} = \frac{\Delta t}{\tau_0}, \qquad \left(\Delta t = \frac{T}{2}\right)$$

The actual value of the maximum is found by inserting this result in the above expression for ξ_1:

$$\xi_1\left(\frac{t}{\tau_0}\right)_{max} = \xi_1\left(\frac{T}{2\tau_0}\right) = \frac{2\tau_0}{T}\tan^{-1}\left(\frac{T}{2\tau_0}\right)$$

or:

$$\xi_1\left(\frac{TS}{BW}\right) = \frac{BW}{TS}\tan^{-1}\left(\frac{TS}{BW}\right)$$

Note that the parameter TS/BW represents the ratio between the averaging time, T, and the swept half power width of the resonance.

To obtain only small errors in the response measurements one must either use a very slow sweep speed ($S \to 0$) or a very small averaging time ($T \to 0$). *In practice therefore, a certain error will always be present when the automatic sweep technique is used for the measurement of resonant responses.*

If RC-weighted averaging is used instead of the running integration technique the output from the averager will take the form:

$$\xi_2\left(\frac{t}{\tau_0}\right) = \frac{\tau_0}{RC}\exp(-t/RC)\int_{-\infty}^{t} \frac{\exp(\tau/RC)}{1+(\tau/\tau_0)^2}\, d\left(\frac{\tau}{\tau_0}\right)$$

This integral cannot be solved readily and use was made of numerical techniques and digital computation, and the results are shown in Fig. 16 of the main text.

To analyze the behaviour of the averaging process in the case of "valleys" in the response characteristic assume that response valleys can be described mathematically by an expression of the type:

$$f(\tau) = 1 + \tau^2$$

or

$$f\left(\frac{\tau}{\tau_0}\right) = 1 + \left(\frac{\tau}{\tau_0}\right)^2$$

Considering now the case of running integration (averaging):

$$\xi_3\left(\frac{t}{\tau_0}\right) = \frac{\tau_0}{T}\int_{(t-T)/\tau_0}^{t/\tau_0}\left[1 + \left(\frac{\tau}{\tau_0}\right)^2\right] d\left(\frac{\tau}{\tau_0}\right)$$

$$= \frac{\tau_0}{T}\left[\frac{T}{\tau_0} + \frac{1}{3}\left(\frac{t}{\tau_0}\right)^3 - \frac{1}{3}\left(\frac{t-T}{\tau_0}\right)^3\right]$$

The minimum of this function occurs when $t = T/2 = \Delta t$ and the value of the minimum becomes:

$$\xi_3\left(\frac{TS}{BW}\right) = 1 + \frac{1}{3}\left(\frac{TS}{BW}\right)^2$$

In the case of RC-weighted averaging one obtains:

$$\xi_4\left(\frac{t}{\tau_0}\right) = \frac{\tau_0}{RC}\exp(-t/RC)\int_{-\infty}^{t}\left[1 + \left(\frac{\tau}{\tau_0}\right)^2\right]\exp(\tau/RC)\, d\left(\frac{\tau}{\tau_0}\right)$$

$$= 1 + \left(\frac{t}{\tau_0}\right)^2 - \frac{2t}{\tau_0^2}(RC) + 2\left(\frac{RC}{\tau_0}\right)^2$$

The minimum value of the function occurs when:

$$\frac{2t}{\tau_0^2} - \frac{2RC}{\tau_0^2} = 0$$

i.e. when $t = RC = \Delta t$, and the value at minimum, setting $RC = T/2$, becomes:

$$\xi_4\left(\frac{TS}{BW}\right) = 1 + \left(\frac{TS}{BW}\right)^2$$

APPENDIX C

On the Performance of a Practical Analog RMS Detector

There exists a wide variety of types of circuits by means of which the root-mean-square (*RMS*)-value of a voltage can be measured. As the name implies such devices are designed to perform a squaring operation, time-averaging, and a squarerooting operation.

Although all these operations are straight forward mathematical manipulations the physical devices designed to perform the operations may take many forms. In the following some details on the actual operation of two types of analog *RMS*-detectors, the direct type and the feedback type, are given.

Consider first a device giving the desired relationship for the squaring of an input voltage, V. Such a device should produce, f.inst. a current, i, which is proportional to V^2 i.e.: $i =$ const. V^2.

Mathematically this describes a parabola:

$$i = pV^2$$

In Fig. C.1 a set of parabolas, all having different parameters, p, are shown:

$$(p = 1\ ;\ p = \tfrac{1}{2}\ ;\ p = \tfrac{1}{5} \quad \text{and} \quad p = \tfrac{1}{10})$$

If the physical device used to perform the squaring is of the socalled "direct" type then the parameter, p, is fixed for all input voltages and a relationship of the kind:

$$i = p_0 V^2$$

exists.

As an example choose $p_0 = \frac{1}{4}$, Fig. C.1. An input voltage of say 2 volts would then produce an output current of say 1 mA. Similarly an input voltage of 4 volts would produce an output current of 4 mA, and an input voltage of 1 volt would produce an output current of 0.25 mA.

By feeding the output current of the device to an *RC* circuit, Fig. C.2, the following differential equation can be derived:

$$i = i_1 + i_2$$

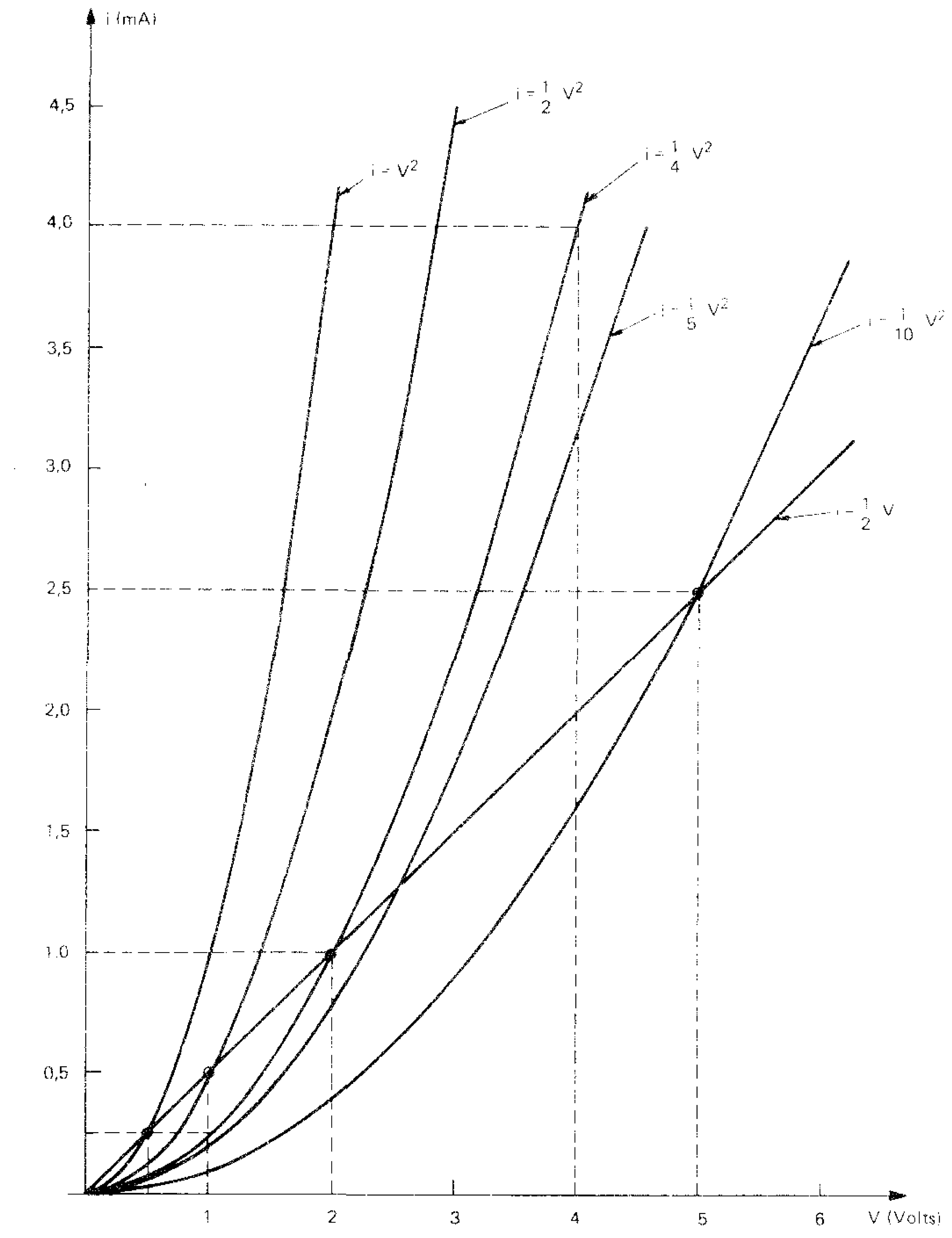

Fig. C.1. Examples of parabolas with different parameters, p.

$$i = p_0 V^2 = \frac{U'}{R_1} + C\frac{d(U')}{dt}$$

where R_1 is the effective resistance of the R-C circuit including the resistance of the indicating meter.

Now, U' will be related to V^2 and it would therefore be more convenient to set $U' = U^2$ to have U represent a linear quantity.

The differential equation would then read:

$$p_0 V^2 = \frac{U^2}{R_1} + C\frac{d(U^2)}{dt}$$

or

$$k_1 V^2 = U^2 + R_1 C\frac{d(U^2)}{dt}$$

where $k_1 = \text{const.} = p_0 R_1$.

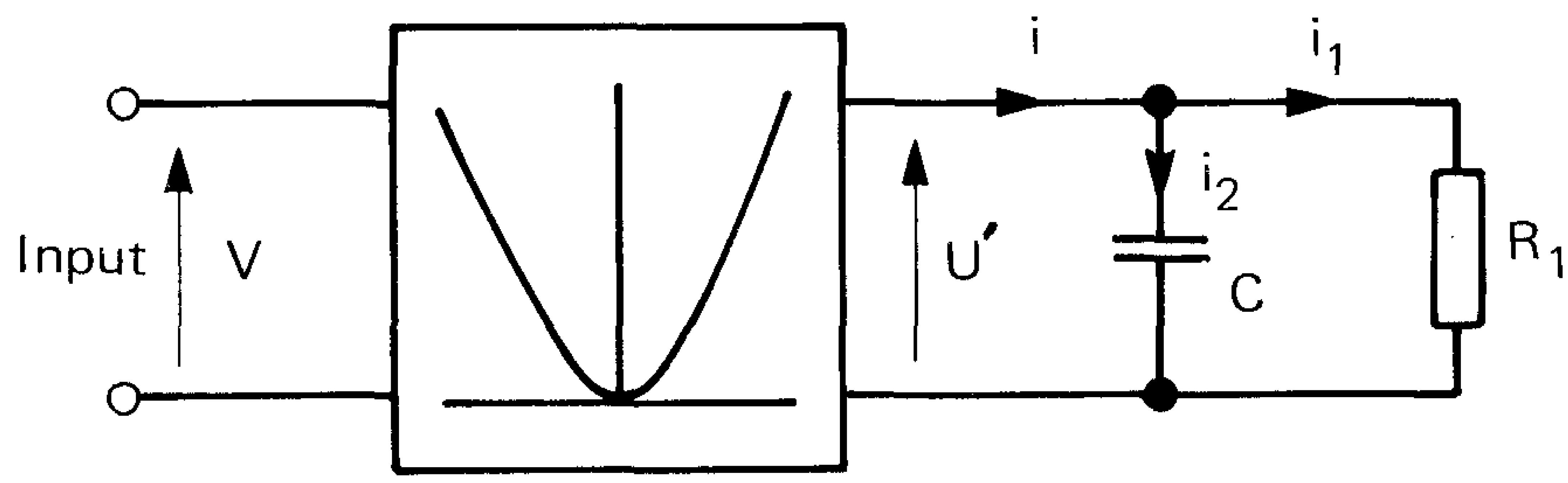

Fig. C.2. Sketch illustrating how the differential equation governing the output from a squaring device ("direct" type) can be derived.

To illustrate the significance of the above equation consider first the case where V is a constant voltage (DC). Then $dU'/dt = 0$ and thus $k_1V^2 = U^2$ i.e. U' $(=U^2)$ would be proportional to V^2.

Next, if V is an alternating voltage (AC) then U' would be proportional *to V^2 averaged over a certain period time* determined by the RC time-constant of the circuit, i.e. U' would be proportional to the mean square value of V.

This is obviously what is required from the circuit.

As $U' = U^2$ a squarerooting operation is necessary to obtain the required *RMS*-value. Normally, this is done by calibrating the instrument meter accordingly, thus obtaining a non-linear meter operation.

A squaring circuit of the direct type can be approximated by means of diodes and resistor as indicated in Fig. C.3a). Here the diodes are permanently biased by means of a fixed voltage (DC) so that they will conduct only when their respective input voltages exceed the bias voltage.

As the input voltage (V) increases more and more diodes become conducting, thereby reducing the effective circuit resistance and increasing the load current. By proper design of the circuit the increase in current can be made very closely proportional to V^2, see also Fig. C.3b). It is clearly seen from Fig. C.3 that in this case only one parabola is used, for the squaring operation, and that the larger the input voltage is the larger is the portion of the fixed parabola which is utilized.

Now, what happens if the diode bias voltages are made proportional

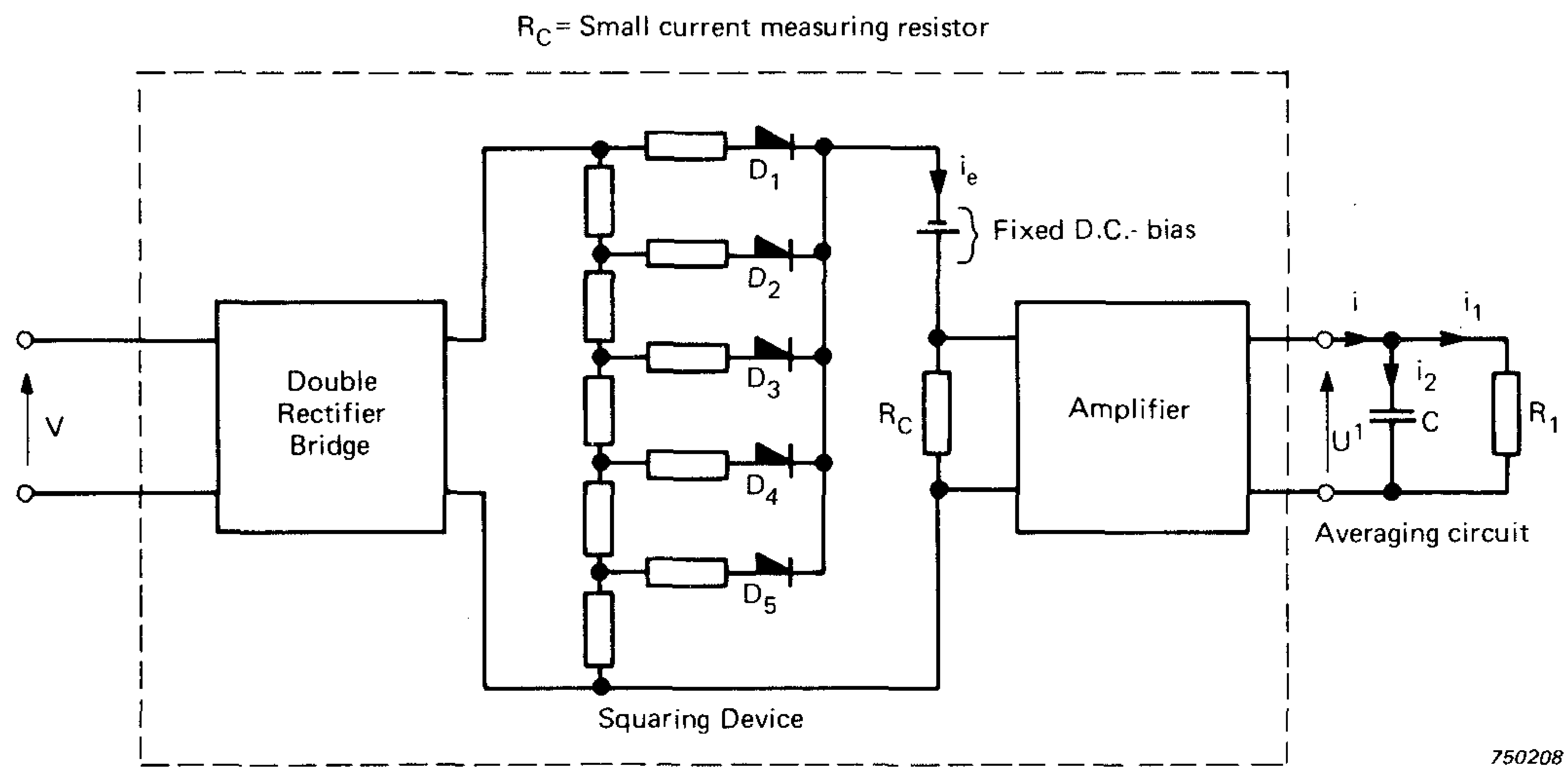

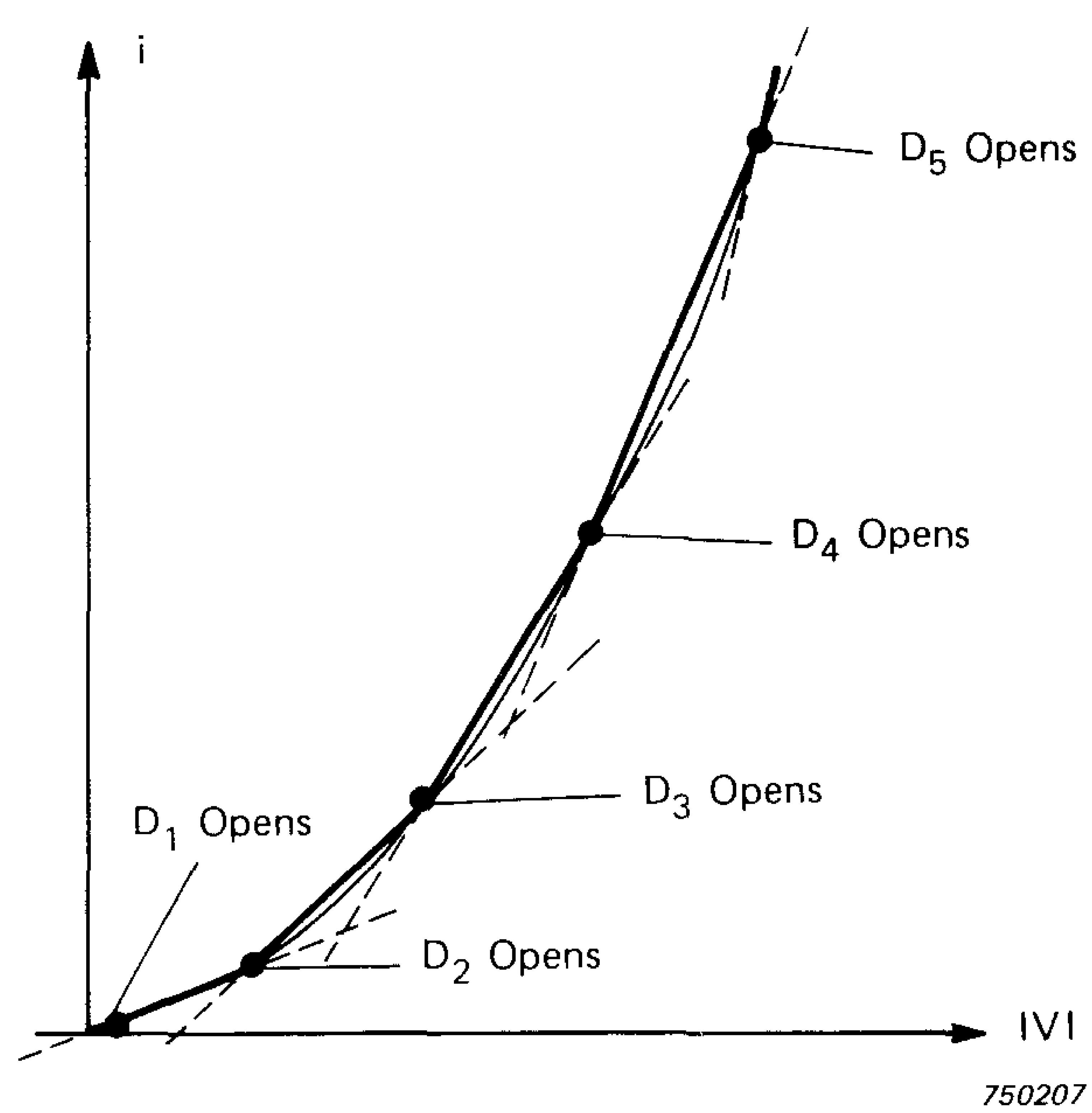

Fig. C.3. Sketches indicating how the parabolic characteristic of the squaring device can be approximated.
a) In terms of electronic circuitry.
b) In terms of output (i) vs. input (| V |) data.

to the output voltage on the capacitor, *C*, i.e. the voltage on the capacitor is fed back into the squaring circuit?

In this case every point on the approximated parabola is projected onto a point on a new parabola with origo as the center of projection, see Fig. C.4. A practical circuit operating according to the described principle is shown in Fig. C.5.

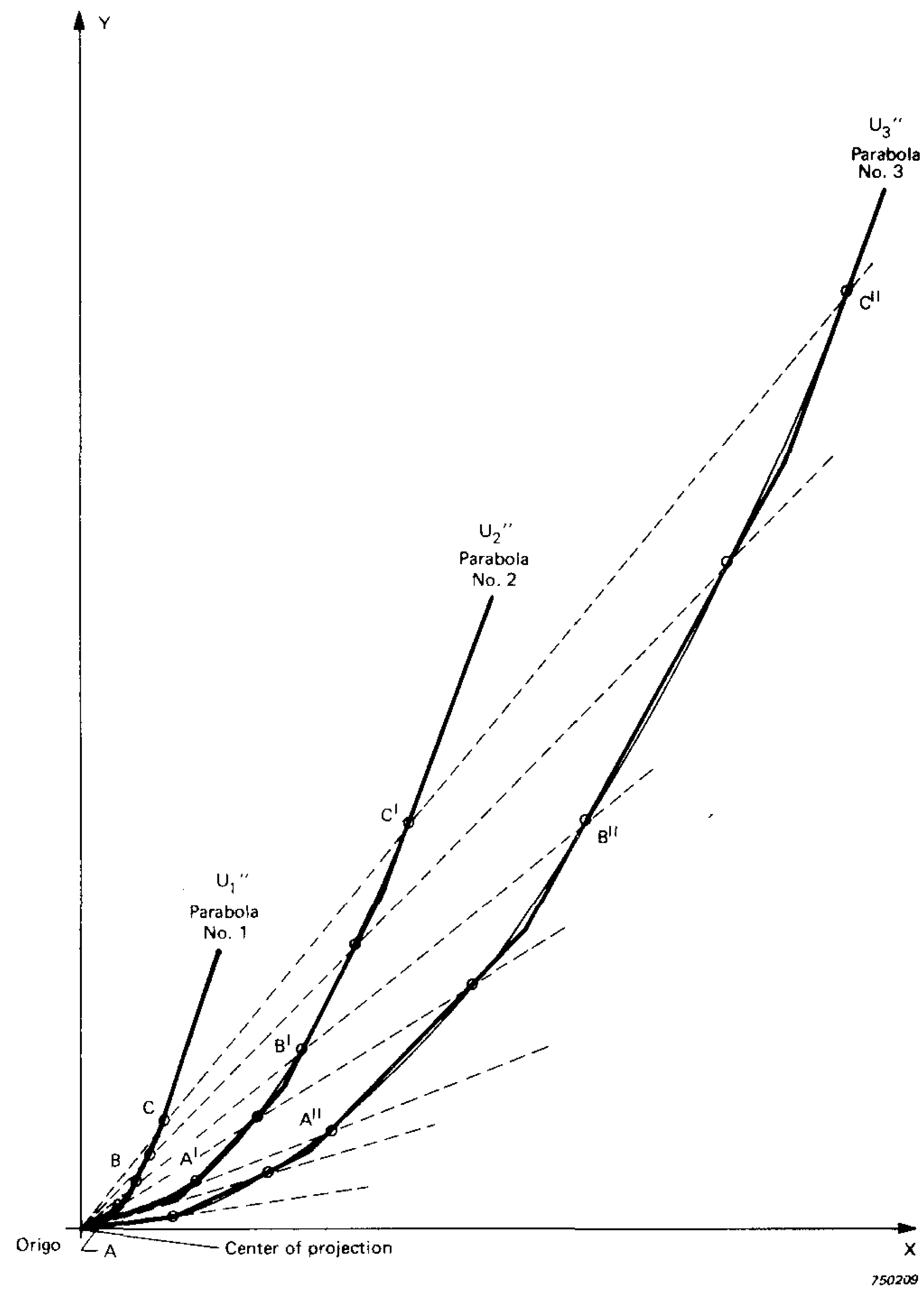

Fig. C.4. Principle of operation of the "feed back" type RMS-detector, illustrating what is sometimes termed a "gliding parabola".

Mathematically the feed back-principle can be described in terms of a parabola with varying parameter, p. As the parabola becomes wider the larger the voltage U'' on the capacitor becomes, the parameter p must vary inversely proportional to U'', see also Fig. C.1. This means that:

$$p = \frac{\text{const.}}{U''}$$

An example readily illustrates this statement.

Assume for instance that $U'' = 2{,}5$ volts, the average output current 2,5 mA and the corresponding operating parabola is $i = \frac{1}{10}V^2$ (Fig. C1.) (i.e. the above const. is 0,25)

The corresponding input could be a DC voltage of 5 vòlts or an AC signal of the same RMS value.

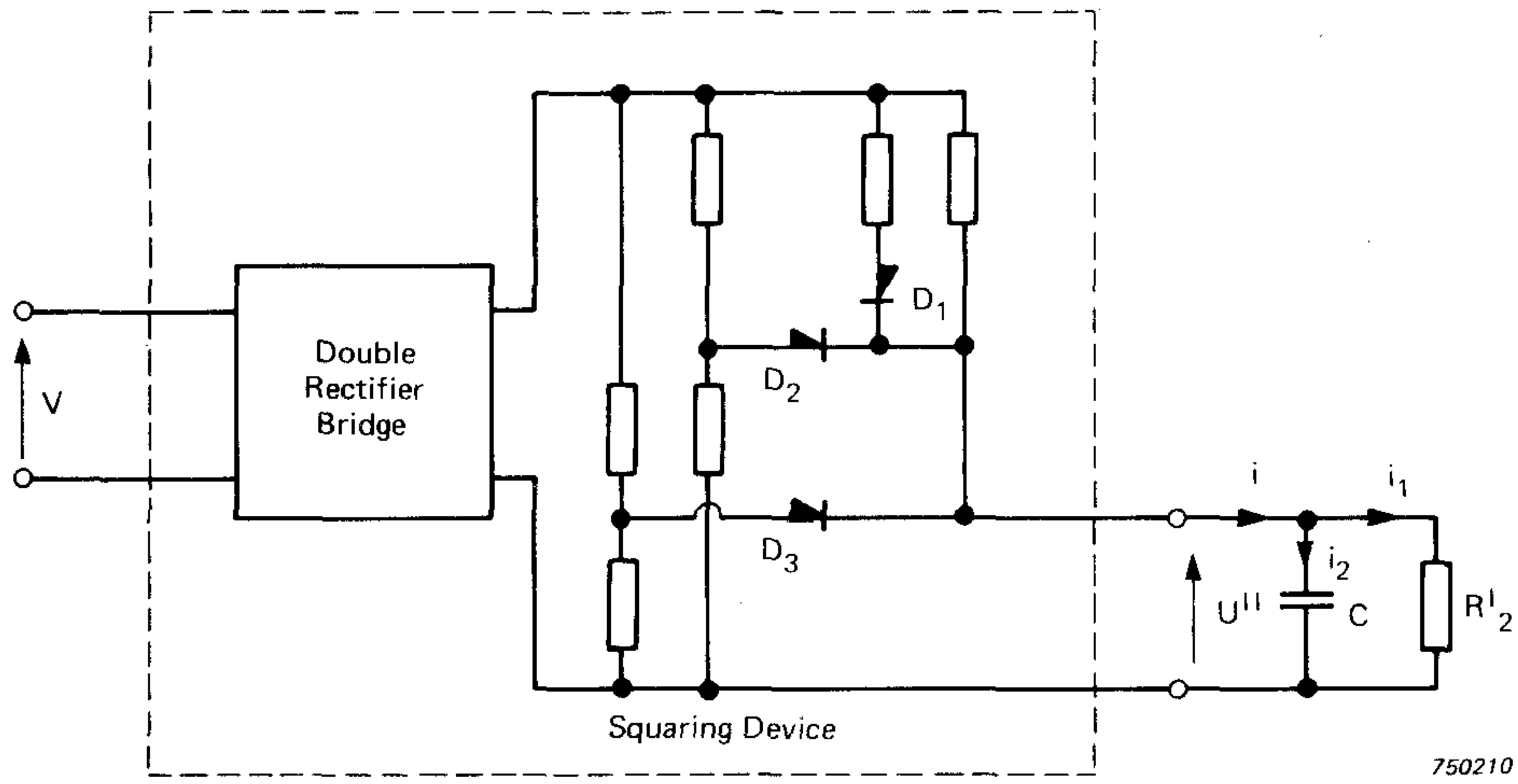

Fig. C.5. Example of an electronic circuit used to produce a "gliding parabola" type of output vs. input characteristic.

If the input signal level is reduced, U'' will gradually follow. Assume that the new level is such that U'' stabilizes at 1 volt. The average output current is proportional to U'' and must therefore be 1 mA and the operating parabola: $i = \frac{1}{4}V^2$. The corresponding input voltage is then 2 volts. In other words: the input signal level, the average output current, and U'' all vary proportionally (for slow changes).

With a ratio of 5 : 2 = 2,5 between the input voltages (and thus also between corresponding U''s) the ratio between the parabola parameters, p, becomes 1/10 : 1/4 = 0,4 = 1/2.5 as predicted by the relationship for p formulated above.

The differential equation governing the operation of the circuit shown in Fig. C.5 therefore becomes:

$$i = i_1 + i_2$$

$$i = pV^2 = \frac{\text{const}}{U''} \cdot V^2 = \frac{U''}{R_2} + C\frac{d(U'')}{dt}$$

or

$$\text{const.} \cdot V^2 = \frac{(U'')^2}{R_2} + \frac{1}{2}C\frac{d[(U'')^2]}{dt}$$

$$k_2 V^2 = (U'')^2 + \frac{1}{2}R_2 C\frac{d[(U'')^2]}{dt}$$

when $k_2 = \text{const.}\ R_2$.

It is readily seen that this equation is of the same type as the one governing the operation of the direct type squaring device, and that the equations become identical (except for k_1 and k_2) if

$$(R_1 C)_{\text{direct}} = \tfrac{1}{2}(R_2 C)_{\text{feedback}}$$

or

$$(RC)_{\text{feedback}} = 2\,(RC)_{\text{direct}}$$

This relationship is quoted in the main text of the paper and does have some implications when the effective averaging time of an *RMS* detection device is measured, as indicated in the following.

A simple method of determining the socalled time-constant (*RC*) of an *RC*-network is to measure the decay of a suddenly interrupted stationary signal. If the decay is measured with a linear time scale and a logarithmic amplitude scale (f.inst. on a logarithmic level recorder) the decay graph becomes a straight line, Fig. C.6. From the slope of the line (dB/sec) the *RC* value can be readily determined:

$$\frac{1}{RC} = \frac{X\ dB/\text{sec}}{8.7}$$

Actual measurements on the Brüel & Kjær Measuring Amplifier Type 2607 (Fig. C.6) showed that with the Averaging Time switch in position "0,3" the decay rate across the capacitor (DC-output) was $X = 28$ dB/sec, and in position "0,1" the corresponding decay rate was 95 dB/sec which gives:

Switch Position	RC
"0,1"	0,0915 sec
"0,3"	0,31 sec

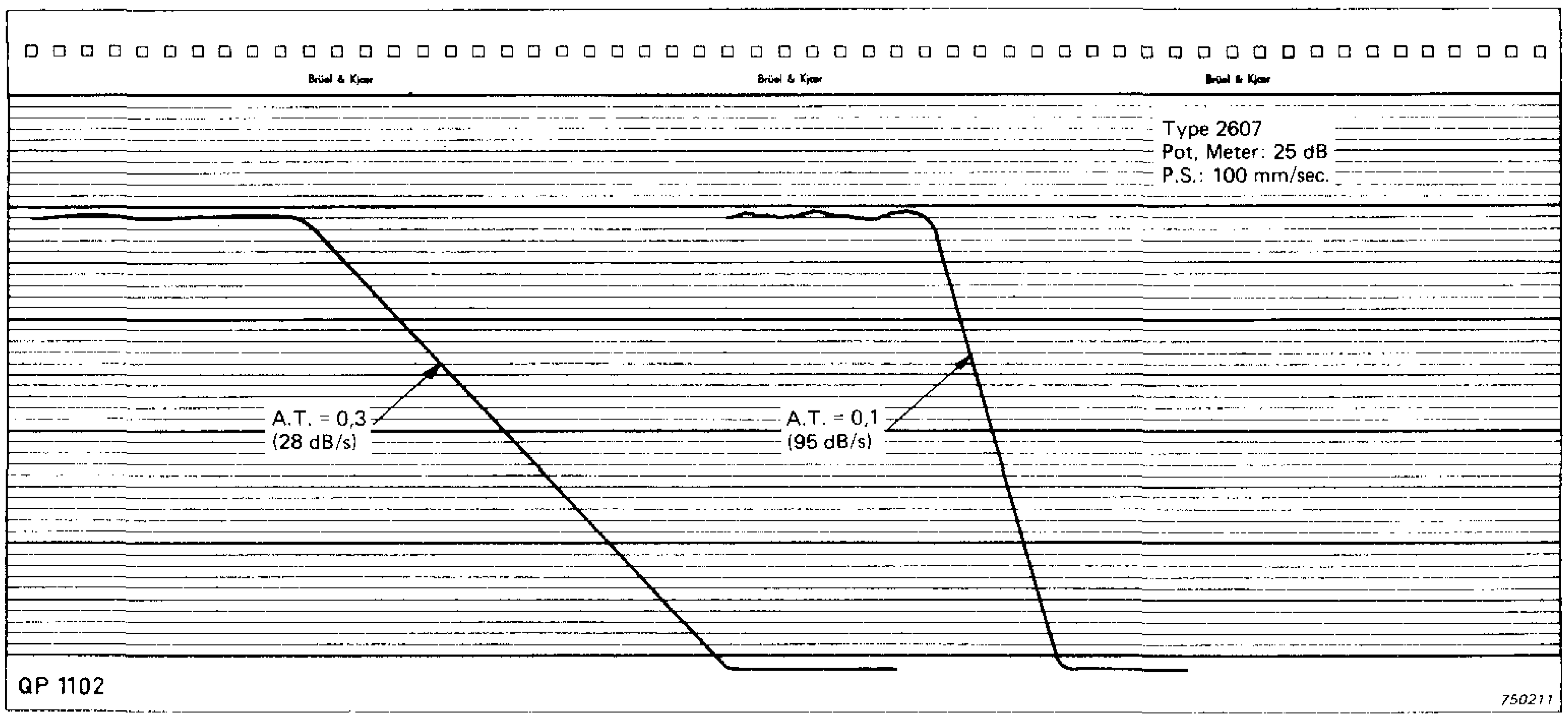

Fig. C.6. Example of measured RC-decays in the averaging circuit of the B & K Measuring Amplifier Type 2607.

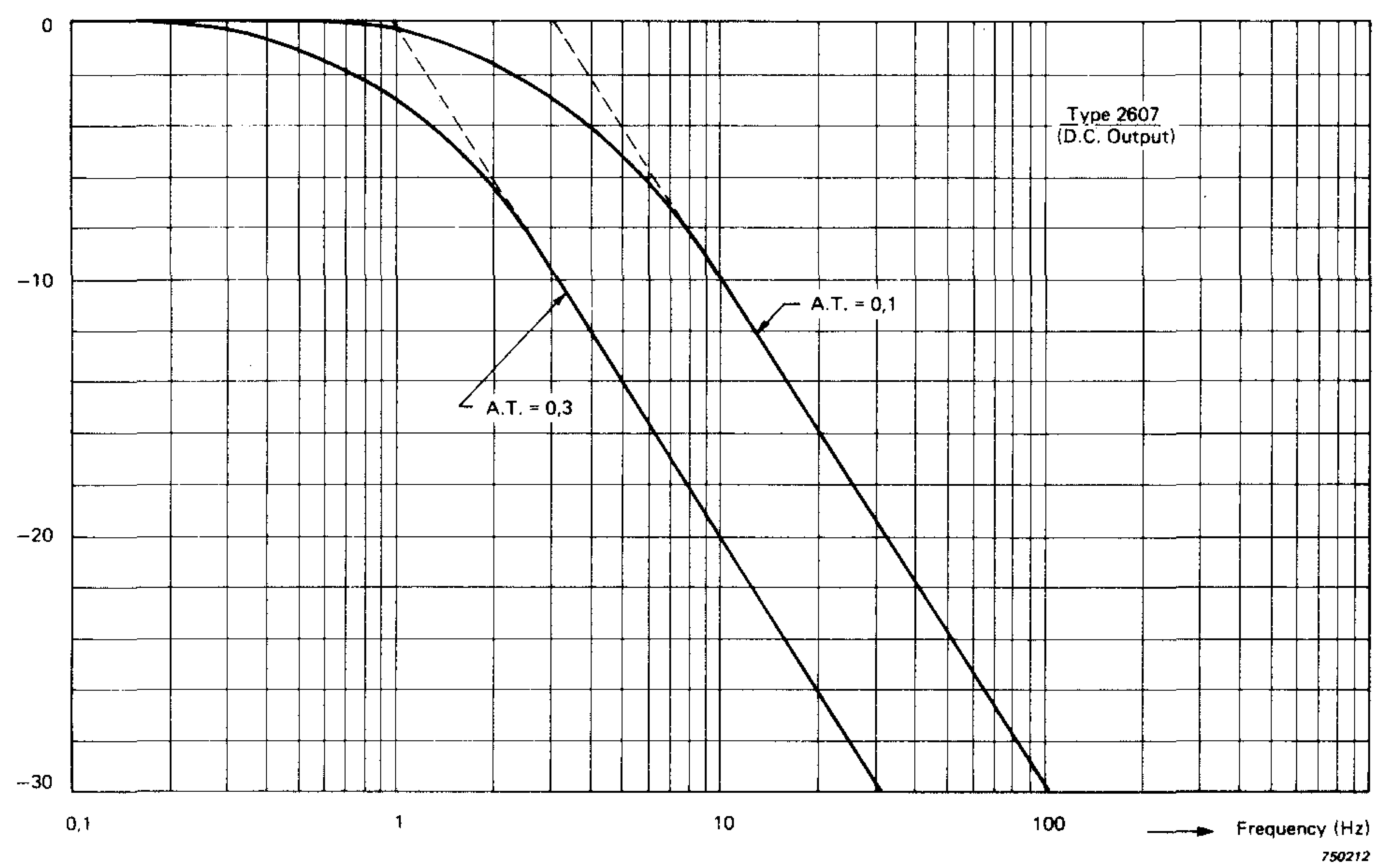

Fig. C.7. Examples of frequency response characteristics of the RC averaging network in the B & K Measuring Amplifier Type 2607.

A second method of measuring the averaging time consists in determining the actual frequency response of the averaging network. This can be done by applying a high frequency signal, amplitude modulated by a variable frequency signal, to the input of the instrument and measuring the response to the modulating signal across the capacitor in the averaging network.

Results, again obtained from measurements on the Type 2607 Amplifier, are shown in Fig. C.7, indicating "corner" frequencies of 3 Hz with the Averaging Time switch in position "0,1", and 1 Hz with the switch in position "0,3".

Using the quoted on p. 13 of the main text in Technical Review No. 2-1975,

$$T = \frac{1}{\pi f_0}$$

then:

Switch Position	Averaging Time
"0,1"	0,105 sec
"0,3"	0,32 sec

As $T = 1/\pi f_0 = 2(RC)_{Eff}$ it is readily seen from the above results that $T = 2(RC)_{Eff} = RC$ or:

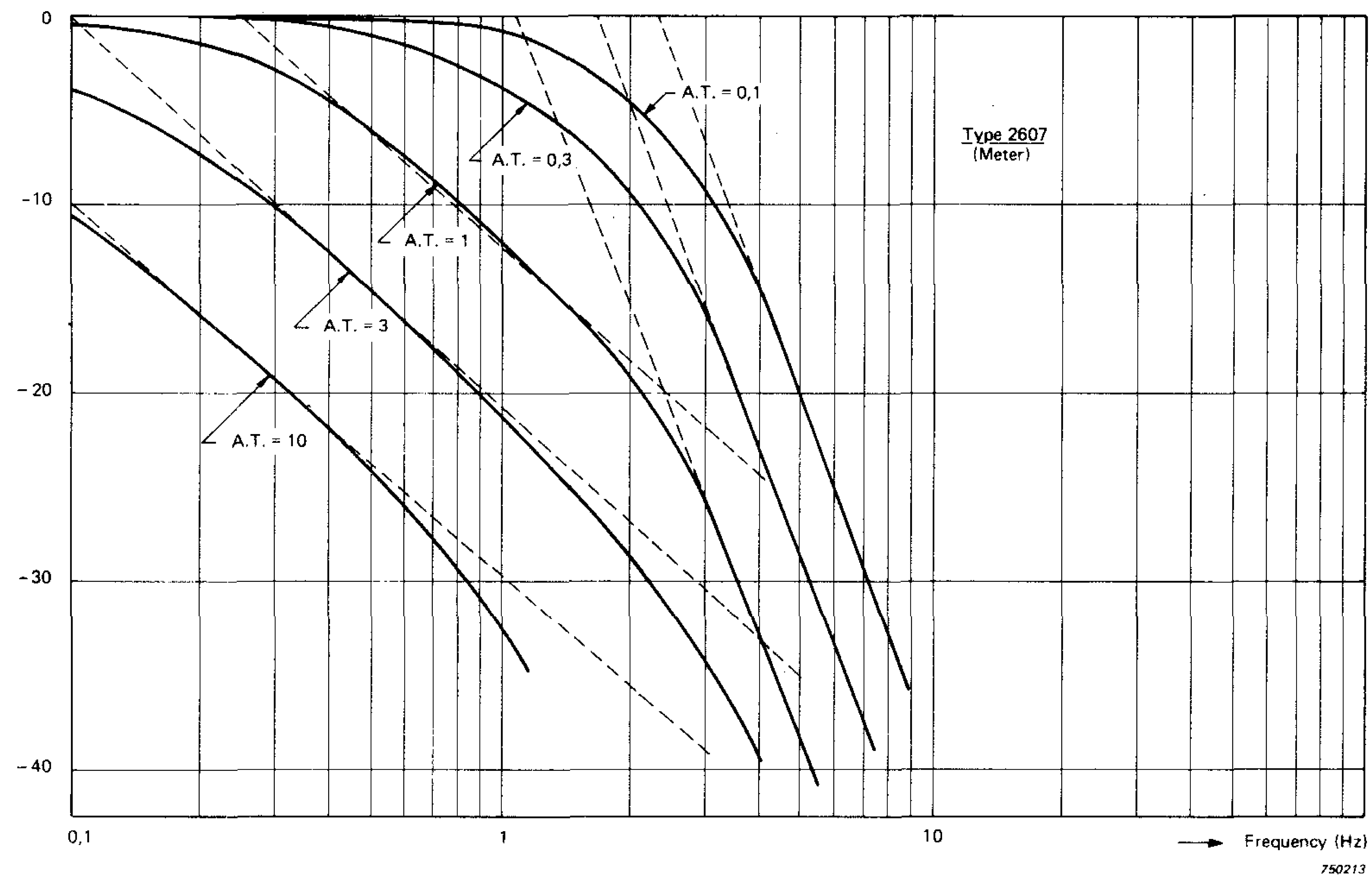

Fig. C.8. Examples of frequency response characteristics measured on the instrument meter of the Type 2607 Measuring Amplifier.

$$RC_{\text{Eff}} \approx \frac{RC}{2}$$

This is in complete agreement with the discussion carried out in the preceding text as the squaring device utilized in the Type 2607 *Amplifier is of the feedback type.*

To illustrate the difference in averaging whether this is done directly by means of an RC-network or on the instrument meter some frequency response measurements were also carried out on the meter using the amplitude modulated input signal technique. The results are shown in Fig. C.8 and indicate that with averaging times of $T = 3$ and $T = 10$ the RC-averaging prevails, while for $T = 1$ and smaller the network properties of the meter play an increasingly important role in the averaging process.

News from the Factory

Shear Accelerometers Types 4366, 4367, 4368, 4369

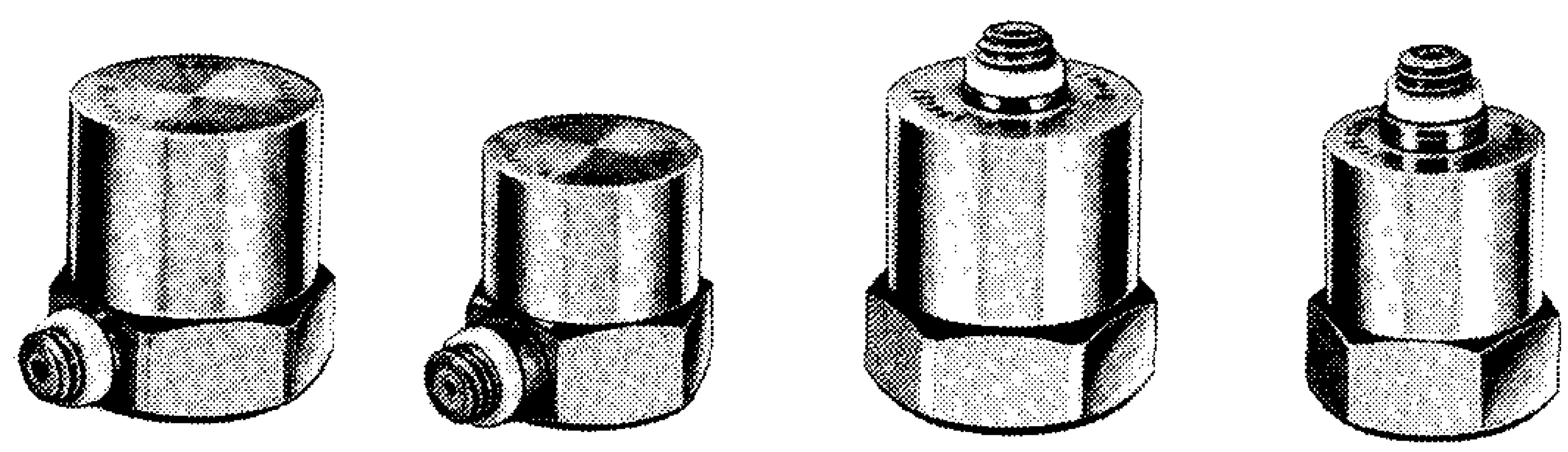

These accelerometers introduced to replace the general purpose accelerometers Types 4332, 4333, 4334 and 4335 respectively, incorporate the new DELTA SHEAR design in which three flat slices of piezoelectric material are clamped between the triangular centre post and individual seismic masses. The mating surfaces of the centre post, the piezoelectric elements and the seismic masses are worked to a fine degree of flatness and held in position by a preloading ring with a very high radial force such that the need of an intermediate layer of adhesive (typically found in annular shear type accelerometers) is avoided. Thus a high degree of amplitude linearity and long term stability is achieved. This design also gives superior performance over the earlier types in exhibiting reduced base strain sensitivity and sensitivity to temperature transients. Types 4366 and 4368 weighing 28 and 30 grams respectively with mounted resonant frequency at 22 kHz, have stainless steel bodies and a typical sensitivity of 4,2 mV/ms^{-2} or pC/ms^{-2}. Types 4367 and 4369 weighing 13 and 14 grams respectively with mounted resonant frequency at 32 kHz have titanium bodies and a typical sensitivity of 2 mV/ms^{-2} or pC/ms^{-2}. Both the stainless steel and titanium types are available with either top or side mounted connectors.

As general purpose accelerometers they are optimized to have good all-round specifications to make them suitable for applications in laboratory, industry and education.

Tunable Band Pass Filter Type 1621

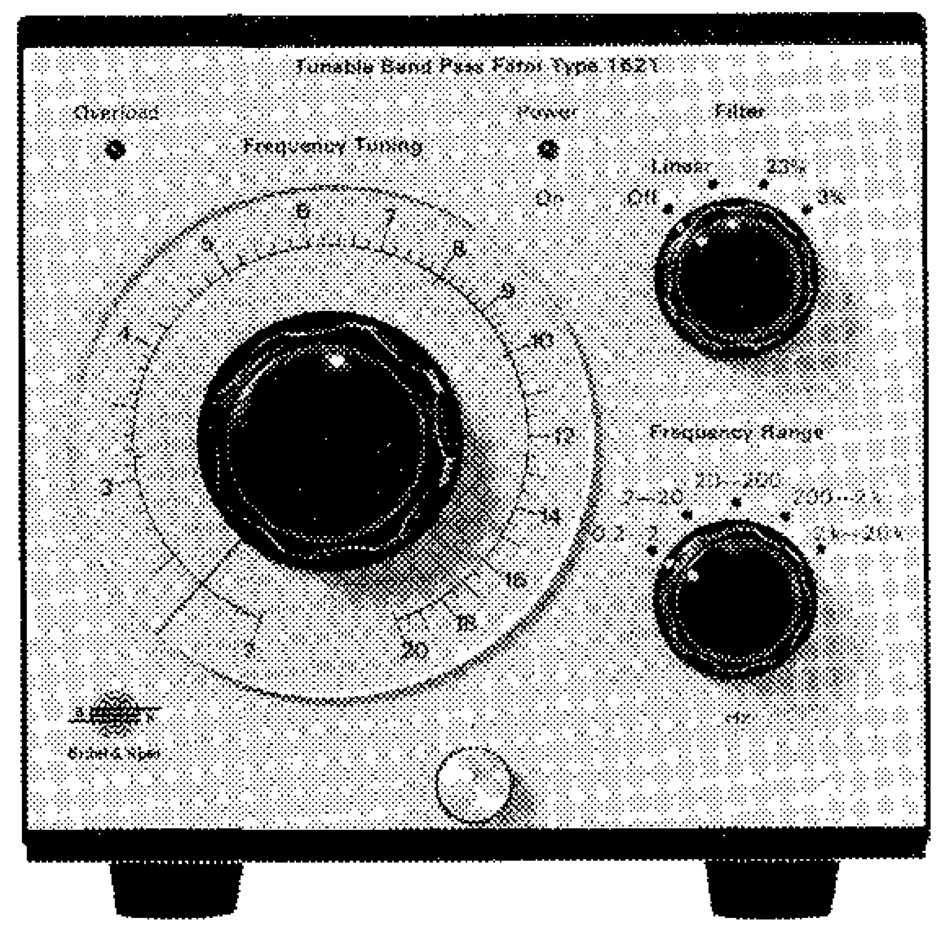

The Tunable Band Pass Filter Type 1621 is a portable instrument intended for use as an external filter with the General Purpose Vibration Meter Type 2511 or Sound Level Meters Types 2203 and 2209 for narrow band frequency analysis of vibration and sound.

The overall frequency range of the filter from 0,2 Hz to 20 kHz is divided into five sub-ranges each covering a decade. The —3 dB filter bandwidth that can be selected are 3% and 1/3 octaves (23%) as well as the linear frequency range in which case the filter is by-passed. When the frequency is swept manually through the sub-range by the frequency indicator knob, the filter can provide a control signal to the Level Recorder Type 2306 for synchronous movement of its paper. Hereby the paper advances at a rate corresponding to the sweep rate of the filter and accurate frequency spectrograms can be plotted.

The power to the filter can be supplied either by internal batteries or by an external DC supply. The standard cells supplied with the instrument would provide 8 to 10 hours of continuous operation while alkaline cells and rechargeable NiCd cells would give continuous operation for 25 to 30 hours and 16 to 20 hours respectively. If an external DC supply is used the voltage required for operation may be between + 4 V and + 12 V or alternatively ± 14 V.

Digital Voltmeter Type 2427

This small size digital voltmeter can measure DC voltages as well as the + Peak, —Peak, Max. Peak, true RMS and Average value of signals of complex waveforms up to a crest factor of 5. It contains an Analog to Digital converter and a Linear to dB converter by which the measured signal can be displayed digitally either in Volts or in dB. The digital seven segment display consists of four digits which in the lowest range

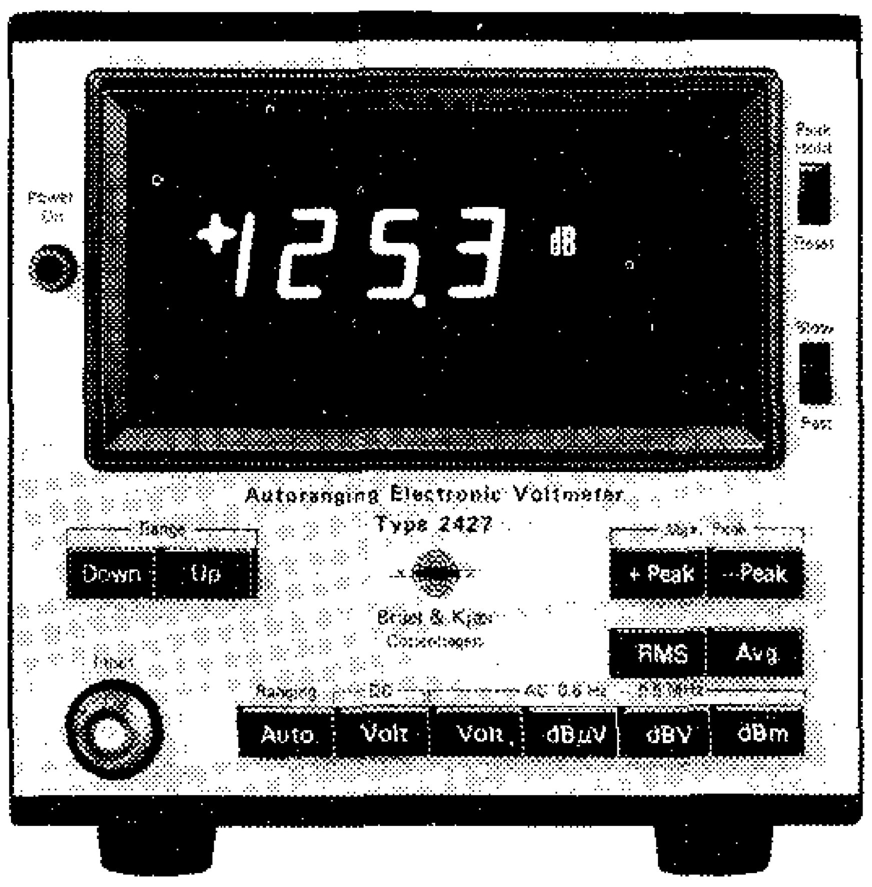

gives a resolution of 10 μV and in the highest range a resolution of 1 V. The displayed value is also available at a BCD output socket. The instrument is extremely easy to operate as in the "Auto" mode it selects the correct range automatically according to the input signal. Finally, a Peak Hold function is also included for measurement on impulsive signals.

The voltmeter can be used as a calibrated amplifier as it has a gain of 60 dB in 20 dB steps and linear AC and DC outputs.

Gating System Type 4440

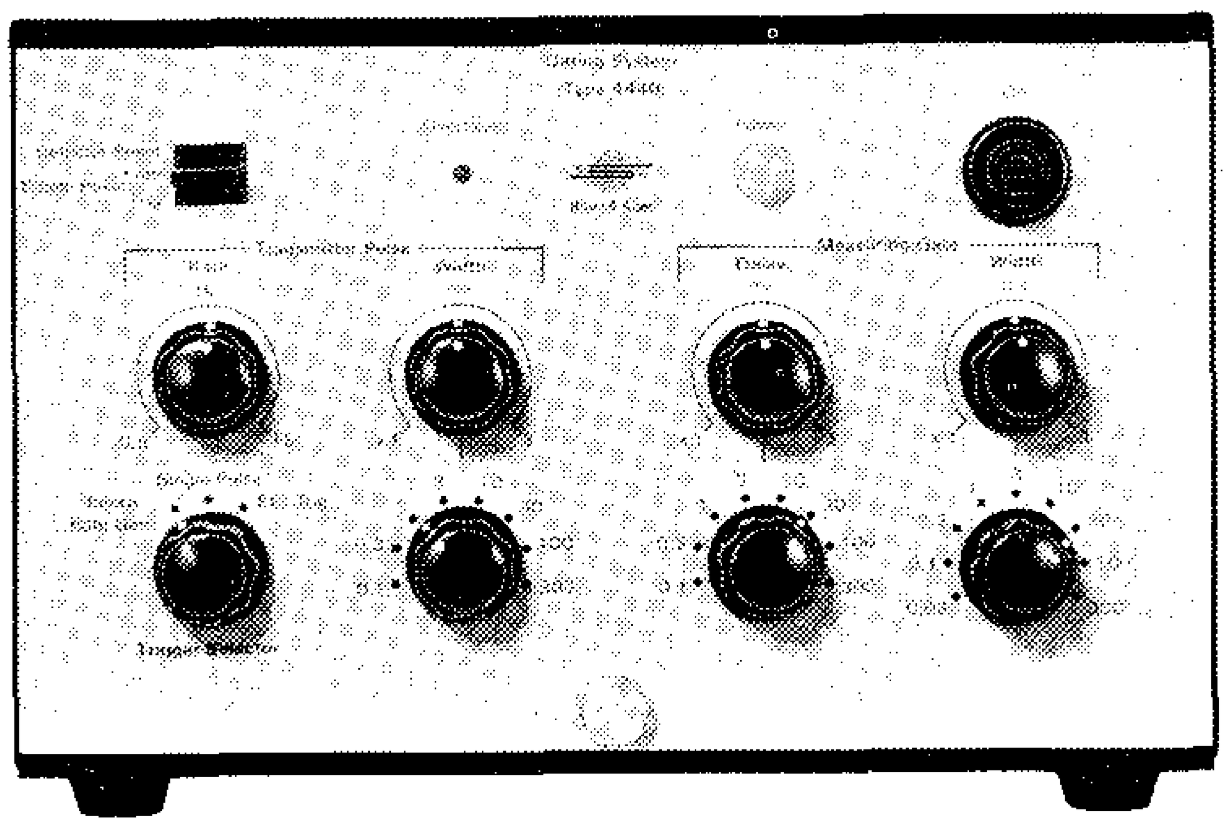

Hydrophones, microphones and loudspeakers normally have to be calibrated under free-field conditions necessitating the use of anechoic water tanks and anechoic chambers which are costly constructions. However, with the use of the Gating System Type 4440 calibration can be carried out even when reflections are present since the echoes caused by the boundaries of the enclosure can be eliminated. This is achieved by emitting an impulse from the transmission section of the Gating System and measuring the received signal only for the period of time during which the direct signal is being received.

The transmission section of the Gating System consists of an Input Amplifier and a MOS Tone Burst Gate which receives the signal from an external generator and emits it as calibrated tone bursts. The width of the pulse can be selected between 0,1 ms and 1,0 s, with the coarse and fine adjustable knobs. The pulse can be triggered either externally or internally in which case the repetition rate can be selected between 0,5 and 15 Hz which is well suited for transducer calibration in air and water. Triggering of single pulses can also be achieved be a spring-off switch on the front panel.

The input signal is also fed to the synchronizing circuit which is the master triggering unit for all time sequences. It not only opens and closes the Tone Burst Gate on a zero crossing point in the input signal to avoid transients and phase distortion but also ensures that the repetition rate never gets shorter than the pulse width.

In the measuring section of the Gating System the synchronizing circuit starts timers in the sequencing logic that control the Measuring Gate delay and Measuring Gate width. With the use of coarse and fine adjustments the Measuring Gate can be delayed between 0,1 ms and 1,0 s and the Gate width can be adjusted between 0,03 ms and 1,0 s. The peak level of the measured signal is sampled and stored in the Hold circuit so that discontinuities in the Level Recorder trace during the "off" period in the duty cycle are prevented. The Hold circuit is reset automatically by the internal logic just before each measuring period.

A low pass filter with a slope of —12 dB/octave over the frequency range 2 Hz to 200 kHz is also included to counteract the 12 dB/octave rise in response to voltage when a piezoelectric hydrophone is used as a projector.

The Gating System can not only be used for calibration of Hydrophones, Microphones and Loudspeakers, but also for automatic recording of their polar and frequency response diagrams. With a calibrated source and receiver the echoes in an enclosure can be examined to determine the absorption and reflection coefficients and the reverberation time. The tone burst generator alone can be used to make performance checks on electronic equipment such as response time of detectors and compressor amplifiers, rise time and hence the bandwidth of tuned circuits, overshoot and recovery time of compressor amplifiers as well as power rating of audio amplifiers.

Reciprocity Calibration Apparatus Type 4143

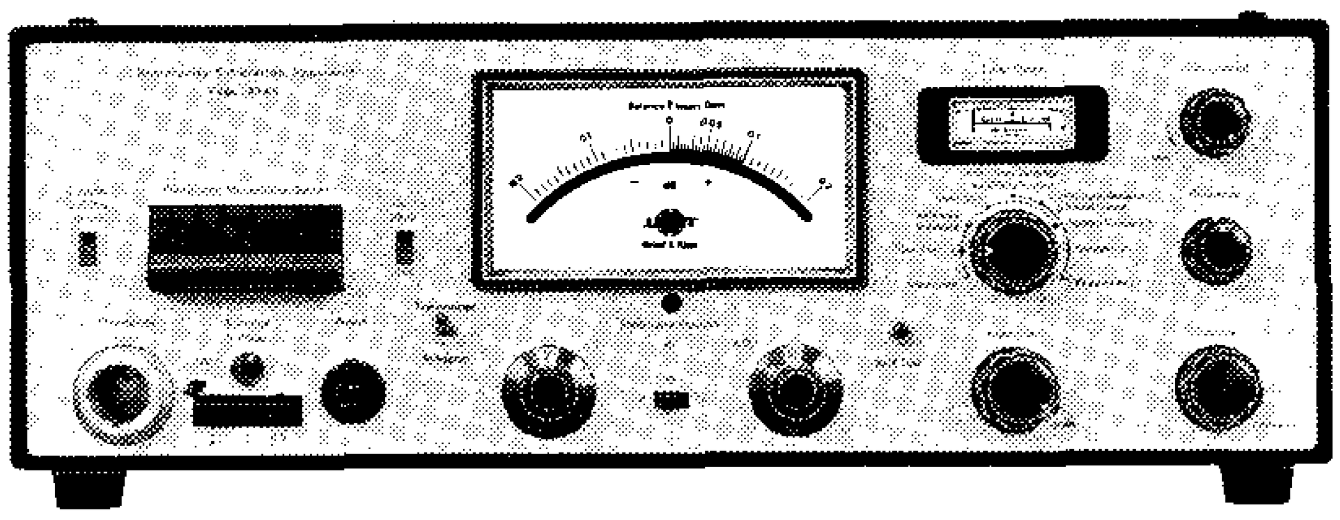

The Reciprocity Calibration Apparatus Type 4143 is a high precision, high stability laboratory instrument designed primarily for precision calibration of condenser microphones by means of the reciprocity method according to IEC Recommendations 327 and 402. It can also be used for comparison calibration of 1" and 1/2" condenser microphones as well as for frequency response measurements of 1", 1/2", 1/4" and 1/8" condenser microphones by the electrostatic actuator method.

The 4143 consists basically of a calibration section and a ratio-voltmeter section interconnected via a function selector. The calibration section contains a coupler base with a transmission microphone socket with standardized ground shield, all mounted in a retractable drawer. This section also contains input and outputs circuits as well as precision polarization voltage supply for the transmitter and receiver microphones. An 800 V DC polarization voltage supply and amplifiers for electrostatic actuator calibration are also included. The ratio-voltmeter section consists essentially of two measuring channels terminating into the main meter. It is used to measure the ratio between the two voltages from the calibration section or between two externally applied voltages. A separate Level Meter is incorporated for aligning the measuring channels and adjusting the calibration section before measuring. A S/N test facility is also included.

The reciprocity and comparison calibration can be carried out in the frequency range 20 Hz to 20 kHz while the microphone calibration range is from —40 dB to —23 dB re. 1 V/Pa.

The instrument is delivered with all the necessary accessories including individually calibrated couplers, a Microphone Preamplifier Type 2627 (with insert voltage facility) and a 1" Condenser Microphone Type 4160.

Finally, the instrument can be used for the measurement of front volume of adaptors, equivalent volume of microphones, reciprocity and comparison calibration of accelerometers as well as a reference sound source and a comparator.

PREVIOUSLY ISSUED NUMBERS OF BRÜEL & KJÆR TECHNICAL REVIEW

(Continued from cover page 2)

SPECIAL TECHNICAL LITERATURE

As shown on the back cover page Brüel & Kjær publish a variety of technical literature which can be obtained free of charge.
The following literature is presently available:

Mechanical Vibration and Shock Measurements (English, German, Russian)
Acoustic Noise Measurements (English, Russian), 2. editon
Architectural Acoustics (English)
Power Spectral Density Measurements and Frequency Analysis (English)
Standards, formulae and charts (English)
Catalogs (several languages)
Product Data Sheets (English, German, French, Russian)

Furthermore, back copies of the Technical Review can be supplied as shown in the list above. Older issues may be obtained provided they are still in stock.

PRINTED IN DENMARK K LARSEN & SØN A/S DK-2860 SØBORG

Brüel & Kjær

DK-2850 NÆRUM, DENMARK · TEL.: (02) 80 05 00 · CABLE: BRUKJA, COPENHAGEN · TELEX: 15316